REMOVAL OF MANGANESE FROM SYNTHETIC WASTEWATER BY ADSORTPION

WENDY KONG YIN JOU

UNIVERSITI MALAYSIA PAHANG

REMOVAL OF MANGANESE FROM SYNTHETIC WASTEWATER BY ADSORPTION

WENDY KONG YIN JOU

Thesis submitted in partial fulfillment of the requirements for the award of the degree of Bachelor of Chemical Engineering

FACULTY OF CHEMICAL ENGINEERING AND NATURAL RESOURCES

UNIVERSITY MALAYSIA PAHANG

FEBRUARY 2013

SUPERVISORS' DECLARATION

We hereby declare that we have checked this thesis and in our opinion, this thesis is adequate in terms of scope and quality for the award of the degree of Bachelor of Chemical Engineering.

Signature :
Name : DR. MD. MAKSUDUR RAHMAN KHAN
Position : ASSOCIATE PROFESSOR
Date : JANUARY 2013

STUDENT'S DECLARATION

I hereby declare that the work in this thesis is my own except for quotations and summaries which have been duly acknowledged. The thesis has not been accepted for any degree and is not concurrently submitted for award of other degree.

Signature :
Name : WENDY KONG YIN JOU
ID Number : KA09082
Date : JANUARY 2013

Special Dedication to Father Lord, my supervisos, my parents,

my family members and my friends for

all your love, care and supports.

ACKNOWLEDGEMENT

In preparing this thesis, I was in contact with many people, researchers and academicians and practitioners. They have contributed towards my understanding and thoughts. I wish to express my sincere appreciation to my supervisor, Associate Prof. Dr. Md. Maksudur Rahman Khan for his encouragement, guidance, critics and also profound advices and motivation throughout the preparation of this thesis.

My sincere appreciation also extends to all the staffs in lab, especially Mr. Mohamad Zaki bin Sahad, Mr. Abd Razak bin Abd Hamid, Mr. Mohd Anuar bin Hj Ramli and others who have provided assistance at various occasions during my experimental works. Their views and tips are helpful indeed. Librarians from University Malaysia Pahang also deserve special thanks for their assistance in supplying the relevant literatures to make this proposal possible.

I would like to express my appreciation to all my friends and family members for their endless love and support. Finally, above all to Almighty God for giving me good health, strength and perseverance to complete this thesis.

TABLE OF CONTENTS

LIST OF TABLES

LIST OF FIGURES

NOMENCLATURE

C_B	Bulk concentration of Mn^{2+} , kg/m^3
Co	Initial concentration of Mn^{2+} , mg/L
Ci/C_T	Relative concentration, mol/L
C_f	Final concentration of Mn^{2+} , mg/L
k_1	Equilibrium constant, min^{-1}
k_1	Lagergen pseudo-first order adsorption rate constant, min^{-1}
k_2	Second order adsorption rate constant, kg/kg.min
K	Langmuir equilibrium constant, m^3/kg
m	Dry weight of adsorbent, kg
m_a	Amount of adsorbent dosage, g
q	Amount adsorbed, kg/kg
q_e	Amount of heavy metal ion adsorbed at equilibrium, kg/kg
q_{max}	Maximum capacity adsorption, kg/kg
q_t	Amount adsorbed at time t, kg/kg
q_∞	Maximum adsorption capacity for Langmuir model, kg/kg
R	Percentage removal, %
R_L	Type of adsorption isotherm
t	Time, min
V	Volume of aqueous phase, m^3
w_a	Adsorbent dosage , kg

PENYINGKIRAN MANGAN DARI SINTETIK AIR MENGGUNAKAN PENJERAPAN

ABSTRAK

Logam berat dianggap sebagai pencemar dalam pelbagai industri dan merupakan masalah alam sekitar yang serius. Industri membebaskan jumlah logam berat yang banyak dan kepekatan tinggi ke dalam air. Apabila menggunakan air bawah tanah sebagai air minuman, penyingkiran mangan telah menjadi masalah terutamanya di bandar-bandar besar. Objektif penyelidikan ini adalah untuk mensintesis dan menentukan cirri-ciri MOCZ untuk penyingkiran Mn^{2+} dari sintetik sisa air dengan mengetahui hubungan masa yang dijalankan, kandungan MOCZ, pH, kepekatan Mn^{2+} yang berbeza terhadap kapasiti penjerapan. Keseimbangan data ditentukan dengan menggunakan Langmuir dan modified Langmuir model. Ciri-ciri MOCZ yang ditentukan termasuk keluasan permukaan MOCZ, isipadu liang, sifat morfologi dan komposisi mineralogy MOCZ dengan masing-masing menggunakan BET, FESEM dan XRD. Penjerapan eksperimen telah dijalankan dengan kepekatan Mn^{2+} yang berbeza dari 50mg/L hingga 200 mg/L pada kelajuan penggoncang 150 rpm selama 120 minit. Dari hasil yang diperolehi, MOCZ mempunyai darjah penghabluran yang rendah, dan oksida yang disalut pada permukaan zeolite adalah vernadite (δMnO2) dengan keluasan permukaan 39.9 m^2g^{-1} dan purata saiz diameter liang sebanyak 1.1733nm. Keputusan menunjukkan bahawa jumlah penjerah Mn^{2+} meningkat dengan pH dan kandungan MOCZ dan kajian kinetik penjerapan menunjukkan penjerapan Mn^{2+} mengikut model pseudo-tertib kedua. Tambahan pula, two sites one molecule bersesuaian dengan data, menunjukkan penjerapan yang kuat dengan kapisiti penjerapan Mn^{2+} sebanyak 0.9267 meq Mn^{2+} g^{-1}. Keputusan menunjukkan bahawa MOCZ berpotensi baik sebagai adsorben Mn^{2+} ion.

REMOVAL OF MANGANESE FROM SYNTHETIC WASTEWATER BY ADSORPTION

ABSTRACT

Heavy metals are considered as pollutants in variety of industrial effluents and it is considered as a serious environmental problem. Industries release various concentration and amounts of heavy metals into water. However, when using groundwater as drinking water, manganese removal has become a problem especially in big cities. The objectives of this research was to synthesize and characterize of MOCZ for the removal of Mn^{2+} from synthetic wastewater by conducting the effect of contact time, adsorbent dosage, pH and initial Mn^{2+} concentration on adsorption capacity. The equilibrium data were fitted by using Langmuir and modified Langmuir isotherm model. Characterization of MOCZ were including specific surface area, pores volume, morphology properties and the mineralogical composition by using BET, FESEM and XRD respectively. Batch adsorption experiments were studied at different initial concentration from 50 mg/L to 200 mg/L at 150 rpm agitation speed for 120 min. The MOCZ showed low crystallinity degree, and the oxide coated on zeolite surface was presented mainly as vernadite (δMnO2) with specific surface area 39.9 m^2g^{-1} and average pore size diameter of 1.1733 nm. Results showed that the amount of Mn^{2+} adsorbed increased with pH and adsorbent dosage and that the adsorption kinetics study of the Mn^{2+} followed a pseudo-second-order model. Furthermore, the two sites one molecule mechanism fitted well equilibrium data, showing a strong adsorption capacity for Mn^{2+} ions reaching a maximum capacity of 0.9267 meq $Mn^{2+}g^{-1}$. Results found showed that MOCZ showed a good potential as adsorbent for Mn^{2+} ions.

CHAPTER 1

INTRODUCTION

1.1 Background of study

The demand of water has increased tremendously with agricultural, industrial and domestic sectors each consuming 70%, 22%, and 8% of the available fresh water and generate large amount of wastewater containing a number of pollutants (Helmer & Hespanhol, 1997). A government report by United Nations Environment Programme East Asian Regional Coordinating Unit, 1994 found that states such Penang, Perak, Selangor and Melaka consisted of highest concentrations of heavy metal in wastewater. However, almost all major rivers, mudflats and coast water near industrialized sites are polluted. This occurred because of poor sewage disposal systems, lack of treatment technologies and indiscriminate discharge of toxic materials from industries (Fu & Wang, 2010). Furthermore, wastewater treatment process need high capital expenditures as the establishment of the drainage system will cost billions of ringgit to the government. Besides that, it is not easy to purify and it may take years to remove the pollutant (Indah Water Konsortium, 2002).

Heavy metals are considered as pollutants in variety of industrial effluents. The increasing contamination of urban and industrial wastewater by toxic metal ions is a serious environmental problem (Mengistie, et al., 2012). Industries such as metal plating, metal finishing, rubber processing, mining, as well as chemical manufacturing release various concentration and amounts of heavy metals into the surface and ground water (Southichak, et al., 2006). These trace elements are considered as toxic and most of the contaminants are released into the environment in high amount that cause risk to human health (Tiller, 1989).

As far as is known, humans suffer no harmful effects from drinking water containing manganese. However, when using groundwater as drinking water, manganese removal has become a problem especially in big cities (Taffarel & Rubio, 2010). According to the Malaysia Sewage & Industrial Effluent Discharge Standard (2000), the discharge limit for manganese in industries is 0.2 mg/L for standard A and 1 mg/L for standard B. Processing industries such as Lynas and other industries discharge amount of manganese into the river. However, manganese is not easily removed due to its high concentration. Manganese interferes with laundering operation, impacts objectionable stains to plumbing fixture, and causes trouble in distribution systems by supporting growth of iron bacteria (Mengistie, et al., 2012). For human cases, the bad effects of long exposure to manganese may affect the central nervous system as well as lung tissue (Fu & Wang, 2010).

In order to remove heavy metals effectively from wastewater, various process for the treatment have been developed, such as chemical precipitation, ion-exchange, membrane separation and adsorption (Mohan & Singh, 2002). Conventional

treatment for manganese removal generally required the use of strong oxidizing agents such as potassium permanganate, chlorine, hypochlorite, chlorine dioxide or ozone (Teng et al., 2001). Therefore, reactive process (adsorption) should be used for heavy metal removal where the adsorbent used should have chemical reactivity towards heavy metals.

1.2 Problem Statement

Nowadays, the increased disposal of heavy metals in water is due to rapid growth and developments of industries. Industries such as electroplating, metallurgical process, mining, chemical manufacturing industries release various concentrations of heavy metals. Metal ions such as cadmium, chromium, copper, lead, zinc, manganese and iron are commonly detected in both natural and industrial effluents (Sayed et al., 2011). In recent years, this problem has received attention as heavy metals in water can be absorbed by marine and human bodies which cause health risk. At high concentration, heavy metals can considerable effects on the health of living organisms such as carcinogens and mutagens (Fu & Wang, 2010).

A number of technologies can be used in order to remove heavy metals from the contaminated wastewater such as filtration, adsorption, chemical precipitation, ion exchange and membrane separation. However, most of this method might not be efficiency in removing heavy metal at very low concentrations, and could be relatively expensive (Mengistie, et al., 2012). These methods are also not effective due to their secondary effluent impact on the recipient environment (Sharma &

Forster, 1994). For this reason, the uses of low-cost materials for adsorbent of metals from contaminated wastewater have been popular.

Adsorption process provides an attractive and alternative treatment compared to other removal techniques because it is more economical and readily available. Zeolite is one of the common adsorbents used in adsorption process. Zeolites have been used as adsorbents, molecular sieves, membranes, ion-exchangers and catalyst, mainly because zeolite exchangeable ions are relatively innocuous (Taffarel & Rubio, 2008). Thus, zeolites are particularly suitable for removing undesirable heavy metal ions wastewater. In order to improve the adsorption capacity and mechanical strength of zeolite, severals methods have been used to modify natural zeolites by either physical or chemical reactions. Therefore, synthesizing of the adsorbent is a challenge to produce an alternative and effective adsorbent.

1.3 Objectives

The objectives of this research are:

i. To synthesize and characterize of MOCZ for the removal of Mn^{2+} from synthetic wastewater

ii. To study the effect of contact time, adsorbent dosage, pH and initial Mn^{2+} concentration on adsorption capacity

iii. To determine the best correlation to the equilibrium data using Langmuir and modified Langmuir isotherm model

1.4 Scope of research

The scopes of this research are:

i. The effect of contact time on the adsorption capacity which is used to find the equilibrium time

ii. The effect of initial concentration of Mn^{2+} aqueous solution which is 50 mg/L, 100 mg/L, 150 mg/L, 200 mg/L

iii. The effect of pH of Mn^{2+} aqueous solution change where the pH is adjusted at 4, 5, 6, 7 and 8

iv. Characterization of MOCZ in terms of specific surface area, pores volume, morphology properties and mineralogical composition

1.5 Significance of study

The rationales of significances of this study are:

i. To prevent the heavy metal concentration release to the water stream which can cause toxicity that can be potential hazard to human health and environment

ii. To reduce the cost of wastewater treatment by using modified zeolite due to its high abundance and high affinity for metal ions

iii. To improve the current adsorption process in wastewater treatment by using modified zeolite

CHAPTER 2

LITERATURE REVIEW

2.1 Wastewater

Wastewater is any water that has been adversely affected in quality by anthropogenic influence. It comprises liquid waste discharged by domestic residences, commercial properties, industry and agriculture and can encompass a wide range of potential contaminants and concentrations (Salam et al., 2011). The domestic water used for normal activity in homes, businesses and institutions (Helmer & Hespanhol, 1997). The domestic wastewater is readily treatable industrial. The characteristics of industrial wastewater depends on the type of industry using the water .Some industrial wastewaters can be treated the same as domestic wastes without difficulty.

There's may contain toxic substances or high percentages of organic materials or solids which make treatment difficult. In such cases, the industrial plant may have to pretreatment its wastewater to remove these pollutants or reduce them to

treatable levels before they are accepted into a general treatment facility. In most common usage, it refers to the municipal wastewater that contains a broad of spectrum of contaminants resulting from the mixing of wastewaters from different sources.

Wastewater is one of the most serious environmental problems. The major source of water pollution in the country is domestic wastewater discharge. The need for the provision of wastewater collection and treatment facilities has long been identified by government as a part of its efforts to protect the environment and well being of the population. However, when these facilities were handed over to local government authorities to operate and maintain, the concerned government agency had difficulty to manage the facilities in a sustainable manner due to inadequate planning, budgeting and ownership (Indah Water Konsortium, 2002).

According to Malaysia's Environmental Law, Environmental quality act, 1974, Malaysia Environmental Quality (Sewage and Industrial Effluents) Regulations, 1979, 1999, 2000,

Table 2.1 Parameter limits of effluent of standard A and B

Parameter	Standard A	Standard B
Temperature (^{o}C)	40	40
pH value	6.0-9.0	5.5-9.0
BOD5 at 20^{o}C	20	50
Heavy metal (mg/L)		
Mercury	50	0.05
Cadmium	50	0.02
Chromium, Hexavalent	0.005	0.05
Arsenic	0.01	0.10
Cyanide	0.05	0.10
Lead	0.10	0.5
Chromium, Trivalent	0.20	1.0
Copper	0.20	1.0
Manganese	0.20	1.0
Nickel	0.20	1.0
Tin	0.20	1.0
Zinc	1.0	1.0
Boron	1.0	4.0
Other pollutants (mg/L)		
Iron (Fe)	1.0	5.0
Phenol	0.001	1.0
Free Chlorine	1.0	2.0
Sulphide	0.5	0.5
Oil and Grease	Not detectable	10.0

2.1.1 Characteristic of Wastewater

Wastewater can be categorized into two characteristics, which is the physical and chemical characteristic.

2.1.1.1 Physical Characteristic

Characteristics of wastewater are detected through the physical senses: temperature, odor and color. Fresh wastewater is turbid, grayish-white in color and has a musty odor. Small particles of feces and paper are visible in the waste stream, but these will rapidly settle if the wastewater is quiescent. Table 2.2 shows the significant colors of wastewater.

Table 2.2: Significant colors in wastewater (Win, 2003)

Color	Problem indicated
Gray	None
Green, yellow or other	Industrial wastes not pretreated
Red	Blood, other industrial wastes or TNT complex
Red or other soil color	Surface runoff into influent, also industrial flows
Dark brown to black	Hydrogen sulfide
Black	Septic conditions or industrial flows

2.1.1.2 Chemical Characteristic

Wastewater is composed of organic and inorganic compounds as well as various gases. Organic components may consist of carbohydrates, proteins, fats and greases, surfactants, oils, pesticides and phenol. Inorganic components may consist of heavy metals, nitrogen, phosphorus, pH, sulfur, chlorides, alkalinity and toxic compounds (Peavy et al., 1985).

2.2 Treatment for heavy metal removal

There are several methods which have been used for the removal of heavy metals from wastewater such as chemical precipitation, ion exchange, membrane separation and adsorption (Mohan & Singh, 2002).

2.2.1 Chemical Precipitation

Chemical precipitation is the most effective method on removing heavy metal from wastewater. According to Fu & Wang (2011), chemical precipitation method is simple and inexpensive to operate. During precipitation process, the chemical will react with heavy metal ions to form insoluble solid. Then, the precipitates formed can be separated by filtration. However, this method will produce large amount of sludge which can lead to the disposal problem (Iwa Water Wiki, 2010). Ceribasi & Yetis (2010) also mentioned that concentration limits are one of the problems which may cause chemical precipitation process become expensive and ineffective in wastewater treatment. Chemical precipitation will cause serious disposal problem which produce large amount of sludge to be treated. Grandt & Mcdonald (1981) proved that chemical precipitation is not suitable to be used because this method have a major disadvantage to the requirement of large doses of alkaline materials to increase and maintain pH values typically from 4.0 to 6.5 for optimal metal removal.

2.2.2 Ion Exchange

Ion-exchange processes have been widely used to remove heavy metals from wastewater due to their advantages, such as high treatment capacity, high removal efficiency and fast kinetics (Kang et al., 2004). Ion-exchange resin, either synthetic or natural solid resin, has the specific ability to exchange its cations with the metals in the wastewater. Among the materials used in ion-exchange processes, synthetic resins are commonly preferred as they are effective to nearly remove the heavy metals from the solution (Alyuz & Veli, 2009). The most common cation exchangers are strongly acidic resins with sulfonic acid groups ($–SO_3H$) and weakly acid resins with carboxylic acid groups (–COOH). Hydrogen ions in the sulfonic group or carboxylic group of the resin can serve as exchangeable ions with metal cations. The uptake of heavy metal ions by ion-exchange resins is rather affected by certain variables such as pH, temperature, initial metal concentration and contact time (Altun and Pehlivan, 2006). Ionic charge also plays an important role in ion-exchange process.

2.2.3 Membrane Separation

Membrane filtration is a thin layer of material capable of separating substances when a driving force is applied across the membrane. Membrane filtration showed high efficiency of removal of heavy metal, easy operation and also space saving (Fu & Wang, 2011). It also produced less solid waste and chemical consumption. However, Fu & Wang (2011) also found that this method is not suitable to removal heavy metal since it is high cost, complexity process and it will

cause membrane fouling. These statements are supported by Chang & Kim (2005) that membrane filtration will cause the membrane fouling which leads to a frequent cleaning and replacement of membranes and will increase the operating cost. Therefore, the removal efficiency of single metal will decrease since there is present of other metals.

2.2.4 Adsorption

Adsorption process is widely used in wastewater treatment. In adsorption process, one or more components of gas and liquid stream are adsorbed on the surface of a solid adsorbent and a separation is accomplished (Geankoplis, 2008). Application of adsorption process include removal of organic compounds from water, coloured impurities from organics, fructose from glucose using zeolite and fermentation products from fermentor effluents. There are various types of low cost adsorbents which are derived from agricultural waste, industrial by product, natural material, or modified biopolymers (Barakat, 2010). These adsorbents are applied for the removal of heavy metals from metal-contaminated wastewater.

2.3 Adsorbent

There are several types of adsorbents used in adsorption process such as activated alumina, silica gel, activated carbon, molecular sieve carbon, molecular sieve zeolites and polymeric adsorbent (Geankoplis, 2008).

Activated alumina is a synthetic porous crystalline gel, which is available in the form of granules of different sizes having surface area ranging from 200 to 300 m^2g^{-1} (Gupta & Suhas, 2009). Bauxite a naturally occurring porous crystalline alumina contaminated with kaolinite and iron oxide normally having surface area ranging from 25 to 250 m^2g^{-1}. According Geankoplis (2008), hydrated aluminium oxide is activated by heating to drive off the water. It is mainly used to dry gases and liquids.

Activated carbon is the most common adsorbent used and it is usually prepared from coal, coconut shells, lignite and wood. Normally, activated carbon has a very porous structure with a large surface area ranging from 500 to 2000 m^2g^{-1} (Gupta & Suhas, 2009). Studies have shown that activated carbons are good adsorbents for the removal of different types of adsorption process but the used of the adsorbent is restricted due to their highest cost (Fu & Wang, 2011). Also, the activated carbons after their use in wastewater treatment become exhausted and are no longer capable of further adsorbing process. It has to be regenerated for further use in purifying water. Furthermore, the regeneration process will result in a loss of carbon and the regenerated product may have a slightly lower adsorption capacity in comparison with virgin activated carbon. However, Monser & Adhoum (2001) showed in their studies that modified activated carbon enhance the removal capacity for the inorganic pollutants.

Silica gel is incompletely dehydrated polymeric structure of colloidal silicic acid with formula $SiO_2.nH_20$ (Ng et al., 2001). It is prepared by the coagulation of colloidal silicic acid results in the formation of porous and nancrystalline granules of

different sizes. It shows a higher surface area as compared to alumina, which ranges from 250 to 900 m^2g^{-1}. Silica gel exhibits an excellent capacity for adsorption of water up to 35-40% of its dry mass. Gupta & Suhas (2009) mentioned in their papers that the adsorption capacities for silica gel are high, but the drawback is that silica is expensive adsorbent.

Zeolites are important microporous adsorbents, which are found naturally and are prepared synthetically. They are also considered as selective adsorbents and show ion exchange property as well as molecular adsorption (Gupta & Suhas, 2009). Taraffel & Rubio (2010) showed that zeolite is a natural porous mineral described as crystalline hydrated aluminosilicates containing exchangeable alkali and earth alkaline cations such as Na^+, K^+, Ca^+ and Mg^{2+}. The main reason of the interest for natural zeolite-bearing materials is the increasing demand of low-cost ion exchange and adsorbent materials in fields such as pollution control and metal recovery as well as their wide availability on the earth. The price of zeolites itself is considered very cheap which is about US$0.03-0.12/kg depending on the quality of zeolite (Babel & Kurniawan, 2003). Zeolites are particulary suitable for removing undesirable heavy metal ions such as lead, nickel, zinc, cadmium, copper, chromium and cobalt, electroplating effluents and agricultural wastewaters. In order to improve the adsorption performance, increased mechanical strength and resistance to chemical environments, several methods have been used to modify natural zeolites by either physical or chemical reactions.

2.4 Manganese

Manganese is a pinkish-gray, chemically active element. It is a hard metal and is very brittle. It is hard to melt, but easily oxidized. Manganese is reactive when pure, and as a powder it will burn in oxygen, it reacts with water (it rusts like iron) and dissolves in dilute acids.

2.4.1 Characteristic of Manganese

Manganese is one of the most abundant metals in soils, where it occurs as oxides and hydroxides, and it cycles through its various oxidation states. Manganese occurs principally as pyrolusite (MnO_2), and to a lesser extent as rhodochrosite ($MnCO_3$).

2.4.2 Applications of Manganese

Manganese is essential to iron and steel production. According to Lenntech water treatment solution, it showed that at present, steel making accounts 85% to 90% of the total demand. Manganese is a key component of low-cost stainless steel formulations and certain widely used aluminum alloys. Manganese dioxide is also used as a catalyst. Manganese is used to decolorize glass and make violet colored glass. Potassium permanganate is a potent oxidizer and used as a disinfectant. Other application of manganese is manganese oxide (MnO) and manganese carbonate ($MnCO_3$) where first goes into fertilizers and ceramics and the second is the starting material for making other manganese compounds.

2.4.3 Health Effects of Manganese

Manganese is a very common compound that can be found everywhere on earth. Manganese is one out of three toxic essential trace elements, which means that it is not only necessary for humans to survive, but it is also toxic when too high concentrations are present in a human body. When people do not live up to the recommended daily allowances their health will decrease. But when the uptake is too high health problems will also occur.

Manganese effects occur mainly in the respiratory tract and in the brains. Symptoms of manganese poisoning are hallucinations, forgetfulness and nerve damage (Fu & Wang, 2011). Manganese can also cause Parkinson, lung embolism and bronchitis. When men are exposed to manganese for a longer period of time they may become impotent. A syndrome that is caused by manganese has symptoms such as schizophrenia, dullness, weak muscles, headaches and insomnia (Kampa & Castanas, 2008).

Manganese is an essential element for human health. However, shortages of manganese can also cause health effects such as fatness, glucose intolerance, blood clotting, skin problems, lowered cholesterol levels, skeleton disorders, birth defects, changes of hair color and neurological symptoms.

2.4.4 Environmental Effect of Manganese

Manganese compounds exist naturally in the environment as solids in the soils and small particles in the water. Manganese particles in air are present in dust particles. These usually settle to earth within a few days.

According to the Public Health Statement for manganese (2008), humans enhance manganese concentrations in the air by industrial activities and through burning fossil fuels. Manganese that derives from human sources can also enter surface water, groundwater and sewage water. Through the application of manganese pesticides, manganese will enter soils. By referring to the air quality guidelines (2001), when manganese uptake takes place through the skin, it can cause tremors and coordination failures. Laboratory tests with test animals have shown that severe manganese poisoning should even be able to cause tumor development with animals (Kampa & Castanas, 2008).

In plants, manganese ions are transported to the leaves after uptake from soils. When too little manganese can be absorbed from the soil, this causes disturbances in plant mechanisms (Environmental Fact Sheet, 2006). For instance disturbance of the division of water to hydrogen and oxygen, in which manganese plays an important part. Manganese can cause both toxicity and deficiency symptoms in plants (Kampa & Castanas, 2008). When the pH of the soil is low manganese deficiencies are more common. Besides that, highly toxic concentrations of manganese in soils can cause swelling of cell walls, withering of leafs and brown spots on leaves (Singare et al., 2012).

2.5 Selective of heavy metal removal by adsorption

Effective removal of toxic metal in connection with a comprehensive wastewater treatment strategy still remains a major topic of present research. Adsorption is the selective collection and concentration onto solid surfaces of particular types of molecules contained in liquid or gas.

The selection of a wastewater treatment process depends upon (Barakat, 2010):

i. The characteristics of the wastewater. This should consider the form of the pollutant, its suspension, colloidal or dissolved, the biodegradability and the toxicity of the organic and inorganic components

ii. The required effluent quality. Consideration should also be given to possible future restriction such as effluent bioassay, aquatic toxicity limitation.

iii. The costs and availability of land for any given wastewater treatment problem

Adsorption from the liquid phase has been used for removal of contaminants present at low concentration in process stream. Furthermore, many industrial wastes contain organic, which are refractory and which are difficult or impossible to remove by conventional biological treatment processes. These materials can frequently be removed by adsorption on active solid surface.

Adsorption separation processes are widely use in industries, particularly in petroleum refining and petrochemical industries. When the solid fluid contraction operation of adsorption is used to treat a fluid stream on industrial scale, one of the following characteristics has usually been responsible for its selection as one most economical method for treatment (Fu & Wang, 2011):

i. High selectivity of the adsorbent
ii. High concentrating power of adsorbent
iii. Chemical instability of the adsorbate
iv. Restriction it to temperature unsuited for other separations
v. Fluctuating or intermittent supply of the fluid feed

The ability of porous solids to reversibly adsorb large volume of vapors and liquids was recognized of the eighteenth century and early experiments were carried out by Scheela & Fontana (n.d.), but the practical application of this properly to large scale separation and purification of industrial process stream is relatively recent.

The advantages of an adsorption system for controlling water pollution are:

i. Less space
ii. Lower capital investment
iii. Simple design
iv. Easy operation of the equipment
v. Efficient removal of organic waste constituents

The application of adsorption as a mean of separating mixtures into two or more streams, each enriched in a valuable component, which is to be recovered, is a more recent development. The economic incentive has been the escalation of energy prices, which has made the separation of close boiling components by distillation; a costly and an economic process. For such mixture, it is generally possible to find an adsorbent for which the adsorption separation factor is much greater than the relative validity, so that a more economic adsorption separation is in principal possible. However, for an adsorption process to be developed on a commercial scale required the availability of a suitable adsorbent in tonnage quantities at economic cost.

CHAPTER 3

METHODOLOGY

3.1 Overview

This chapter described about the preparation of manganese oxide coated zeolite, the characterization of manganese oxide coated zeolite and the adsorption experiments procedure that has been designed to complete this research project. To accomplish the objectives and scope of this research, the study was carried out into two parts which are characterization of the adsorbent and adsorption studies.

Figure 3.1 showed the flow chart for the design procedure. Zeolite was coated with manganese oxide which was used as adsorbent. Then, characterization of MOCZ was studied by using BET, FESEM and XRD. Next is the adsorption experiments which including effect of pH, adsorbent dosage, contact time and initial concentration.

3.2 Methodology flow chart

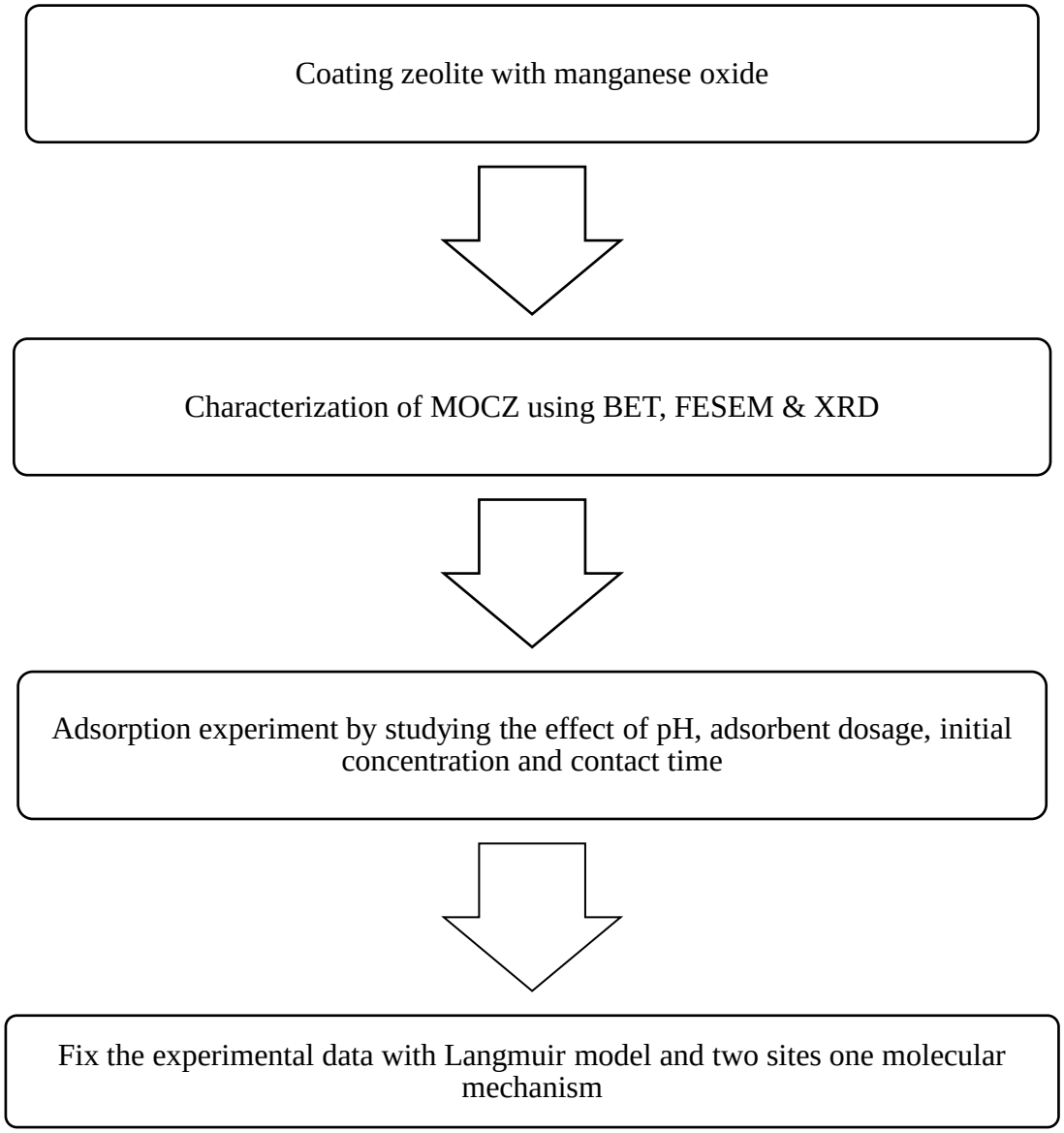

Figure 3.1: Flow chart for designed procedure

3.3 Materials

Table 3.1 showed the list of chemicals used in the experiments with its purity and phase.

Table 3.1: List of Chemicals used

Chemical	Formula Name	Purity (%)	Phase
Sodium Chloride	NaCl	99.5	Solid
Hydrochloric acid	HCl	37.0	Liquid
Potassium permanganate	$KMnO_4$	-	Solid
Sodium hydroxide	NaOH	48-50	Solid
Zeolite (granular)	-	-	Solid
Manganese (II) sulfate monohydrate	$MnSO_4.H_2O$	99	Liquid

3.4 Preparation of MOCZ

The zeolite was converted to its Na form by suspending 30g of zeolite in 500 mL of a 1M NaCl solution for a period of 24 hours. After that, the zeolite suspension was filtered and washed with deionized water. The resulting Na-zeolite was dried in oven at 100 ℃ for 24 hours before use (Taffarel and Rubio, 2009).

MOCZ was prepared utilizing a reductive (Richter et al., 1999) procedure modified to precipitate colloids of manganese oxides onto Na-zeolite surfaces. Manganese oxide was precipitated in aqueous solution by the reaction in equation 1:

$$2KMnO_4 + 8HCl \rightarrow 2MnO_2 + 2KCl + 3Cl_2 + 4H_2O \qquad (1)$$

After that, Na-zeolites samples dried were poured over a heated solution at 90^{o}C, containing potassium permanganate placed in a beaker, followed by dropwise addition of hydrochloric acid (37.5% wHCl/wH2O). After stirring for 1 hour, the suspension was filtered, washed several times using distillated water in order to remove the free potassium and chloride ions. The suspension was dried in oven at 100 ℃ for 24 hour and stored in a polypropylene bottle for use.

3.5 Characterization of MOCZ

3.5.1 Brunauer, Emmett and Teller (BET)

Analyses of the physical characteristics of MOCZ include specific surface area and pore size distributions. The specific surface area of MOCZ and pore volumes were tested using nitrogen adsorption method with a high speed, automated surface area and pore size analyzer, and the Brunauer, Emmett and Teller (BET) adsorption model was used in calculation.

3.5.2 X-ray diffraction (XRD)

The mineralogical composition of MOCZ was determined by using X-ray diffraction (XRD) equipments equipped with Cu Kα radiation.

3.5.3 Field emission scanning electron microscopy (FESEM)

Morphological properties of MOCZ were studied by field emission scanning electron microscopy (FESEM). Micrographs at different magnification were taken to identify the surface morphology after coating with manganese oxide.

3.6 Batch adsorption experiments

Batch adsorption experiments were carried out in 250 mL conical flasks using an orbital shaker at a constant agitation of 150 rpm. Supernatant aliquots were collected, centrifuged and filtered before chemical analysis. Synthetic wastewater samples were prepared by using analytical grade manganese (II) sulfate monohydrate ($MnSO_4.H_2O$) and distilled water. The stock solution was prepared in a concentration of 1000 mg/L. Working solutions of 50, 100, 150, 200 mg/L were prepared by dilution. Manganese ion concentration was determined by using Flame Atomic Absorption Spectrophotometer (AAS) and the results were expressed as mg Mn L^{-1}.

3.6.1 Kinetic studies

3.6.1.1 Effect of contact time

Batch adsorption tests were done at different $MnSO_4.H_2O$ concentration at a constant pH and contact time of 120 min. The initial concentration of Mn^{2+} was measured. The suspensions 1 g of MOCZ and 0.1 L of a 50 mg Mn^{2+} L^{-1} solution

were stirred for different withdraw intervals time (1, 2, 3, 4, 5, 10, 15, 30, 45, 60, 90, 120 min). After adsorption equilibrium was attained, the concentration of the metal ions in the filtrate was determined by AAS. Calibration curve was prepared at different concentration (0.2, 0.4, 0.6, 0.8 and 1.0 mg/L).

3.6.1.2 Effect of initial concentration

The adsorption studies of Mn^{2+} onto MOCZ were conducted using the same procedure during 120 min as it is sufficient for attaining chem. ical equilibrium and varying the feed solution concentration (50, 100, 150, 200 mg/L).

3.6.1.3 Effect of MOCZ dosage

Suspensions 1 g of MOCZ was added into 150 mg Mn^{2+} L^{-1} solution and the solution were stirred for a period of 120 min. After 120 min, the supernatant aliquots were collected and filtered for analysis. The procedure was repeated using 5 g and 7g of MOCZ respectively in 150 mg Mn^{2+} L^{-1}.

3.6.1.4 Effect of pH

The effect of medium pH n Mn^{2+} adsorption was studied by adjusting the initial pH values (4, 5, 6, 7 and 8) before agitation in the orbital shaker. All the ion-exchange results were measured after 120 min.

3.6.2 Equilibrium studies

The equilibrium adsorption experiments were carried out at different concentration 50, 100, 150, 200 mg/L. After 300 min, the aqueous phase was taken, centrifuged and separated from MOCZ, and the concentration of the metal ions in the aqueous phase was measured. The experimental data was fitted by using Langmuir model and two sites one molecules mechanism.

CHAPTER 4

RESULTS AND DISCUSSION

4.1 Characterization of MOCZ

In order to study about the characterization of MOCZ, several analyses have been done using BET, FESEM and XRD. Physical characteristics of MOCZ such as specific surface area and pore size distributions, mineralogical composition and morphological properties of MOCZ have been studied.

4.1.1 Brunauer, Emmett and Teller (BET)

Analyses of the physical characteristics of MOCZ include specific surface area and pore size distributions. The specific surface area of MOCZ and pore volumes were tested using the nitrogen adsorption method and the BET adsorption model was used in the calculation. The specific surface area for MOCZ under adsorbed Mn^{2+} was 39.90 m^2g^{-1} after degassing overnight at 300°C. The pore

specific volume at P/P_o was 0.99 which was showed in Figure 4.1 and Figure 4.2 showed the BET plot for surface area calculation.

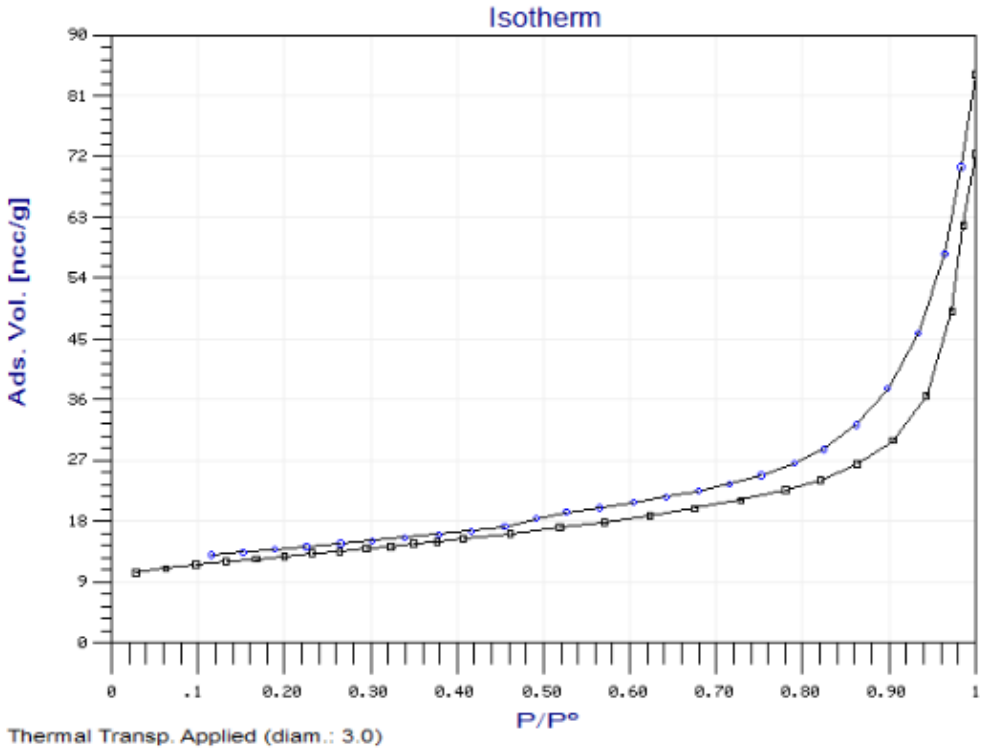

Figure 4.1 Isotherm curve for pore specific volume of MOCZ

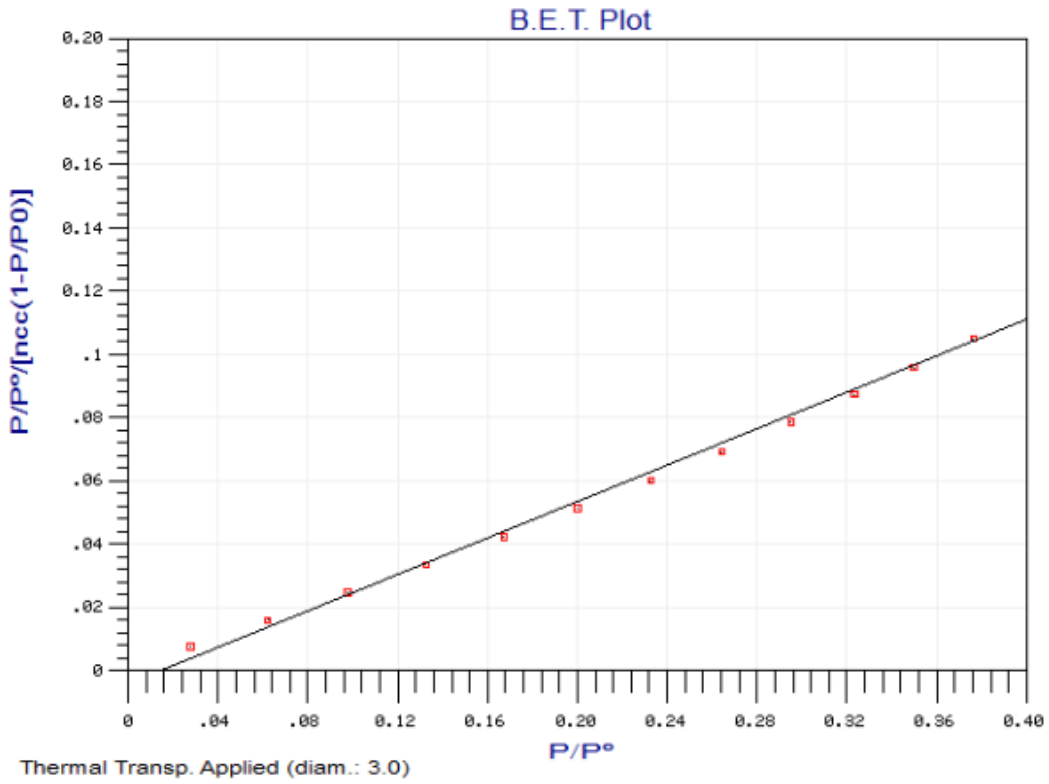

Figure 4.2 BET plot for surface area calculation

4.1.2 Field emission scanning electron (FESEM)

Micrographs shown in figure 4.1 were taken at 14000x magnification to observe the manganese oxide coated zeolite surface morphology by manganese oxides deposition.

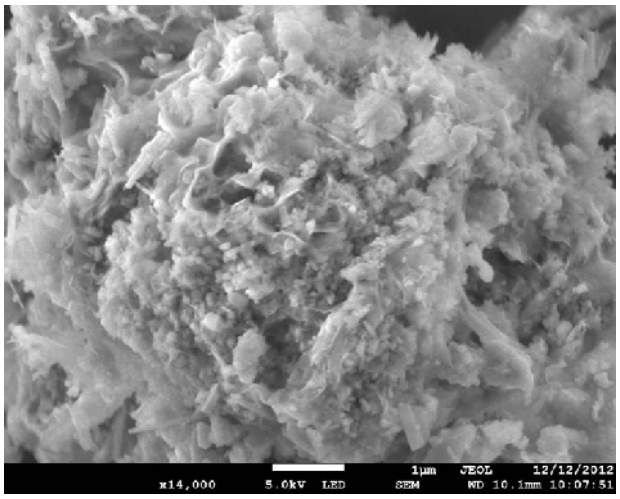

Figure 4.3 FESEM micrograph of MOCZ samples

Figure 4.3 showed that the zeolite surface sites were occupied by newborn manganese oxide, which was formed during the coating process. It also showed that manganese oxide formed as clusters onto the zeolite surface. The synthetic coating is composed of small particles on the surface of a more consolidated coating. It can also be observed that manganese oxide particles (diameter from 1 to 3μm) appear to be growing together in surface depressions and coating cracks.

4.1.3 X-ray diffraction (XRD)

The diffractogram obtained for MOCZ sample is shown in Figure 4.4 and the main mineral phases present in sample MOCZ are modernite, vernadite, quartzo, clinoptilotile and montmorillonite.. The diffractogram of Figure 4.4 showed that MOCZ has a low crystallinity degree, and that the oxide coated on zeolite surface is presented mainly as Vernadite, also referred as δMnO2 (Balistrieri and Murray, 1982).

Table 4.1 Mineral phases present in sample MOCZ

Mineral phases	Molecular formula	Peaks
Mordenite	$(Ca, Na_2, K_2)Al_2Si_{10}O_{24}.7H_2O$	1, 2,
Vernadite	$MnO_2.nH_2O$	4, 5, 7, 8
Clinoptilolite	$(Na,K,Ca)6(Si,Al)_{36}O_{72}.20H_2O$	3,
Quartz	SiO_2	6

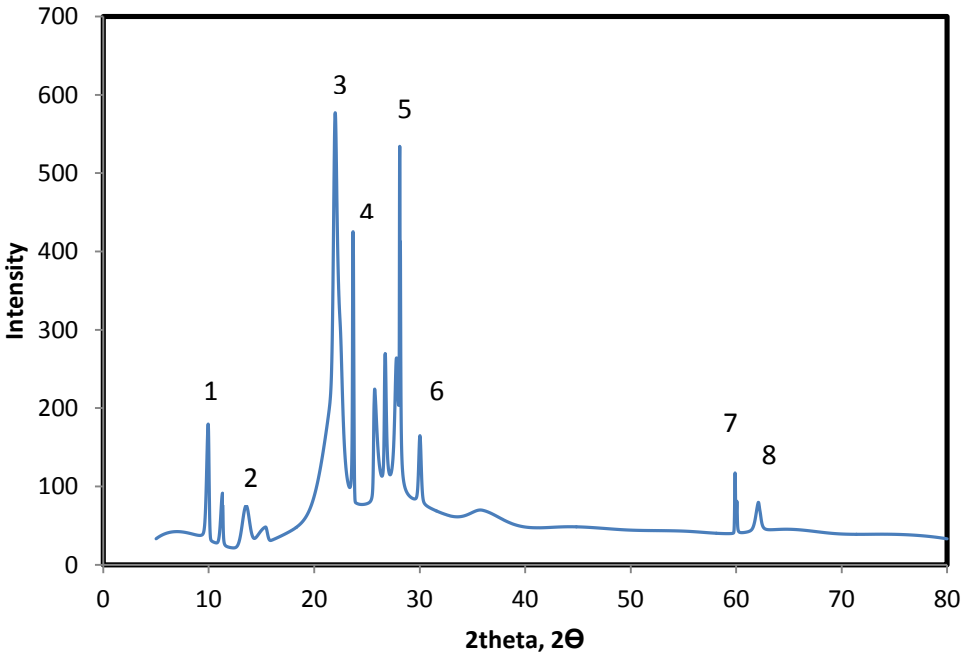

Figure 4.4 X-ray diffractogram of the MOCZ sample

4.2 Adsorption Experiments

Batch adsorption experiments were carried out by shaking the conical flasks at 150 rpm for a period of 120 min using orbital shaker at room temperature. Following a systematic process, the adsorption uptake capacity of Mn^{2+} in batch system was studied.

4.2.1 Effect of initial concentration of MOCZ

The adsorption capacity (kg/kg) and the adsorption of Mn^{2+} at different concentration of MOCZ were represented in Figure 4.5. It was observed that the percentage of Mn^{2+} adsorbed by MOCZ decreased when the adsorbent concentration increased from 50 mg/L to 200 mg/L. Moreover, the plot of amount adsorbed versus adsorbent concentration revealed that the uptake capacity was higher at lower concentration and reduced at higher concentration. The corresponding data were shown in the Appendix B1.

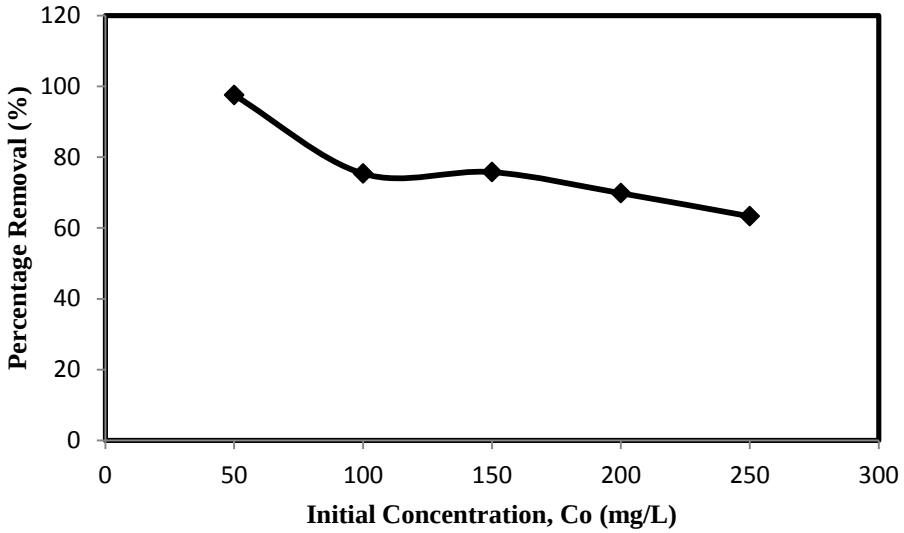

Figure 4.5 Percentage removal of Mn^{2+} with different initial concentration and initial pH 7 and 1 g of MOCZ

4.2.2 Effect of contact time on adsorption of Mn^{2+}

Effect of contact time on adsorption was studied for different initial concentration with fixed adsorbent dosage 1g was used. The amount of Mn^{2+} adsorbed versus time curves was shown in Figure 4.6. The corresponding data were shown in the Appendix B2.

The different initial concentration, the times needed to attain equilibrium and amount of Mn^{2+} adsorbed in adsorbent during equilibrium were different. Both of them increased with increasing the initial concentration.

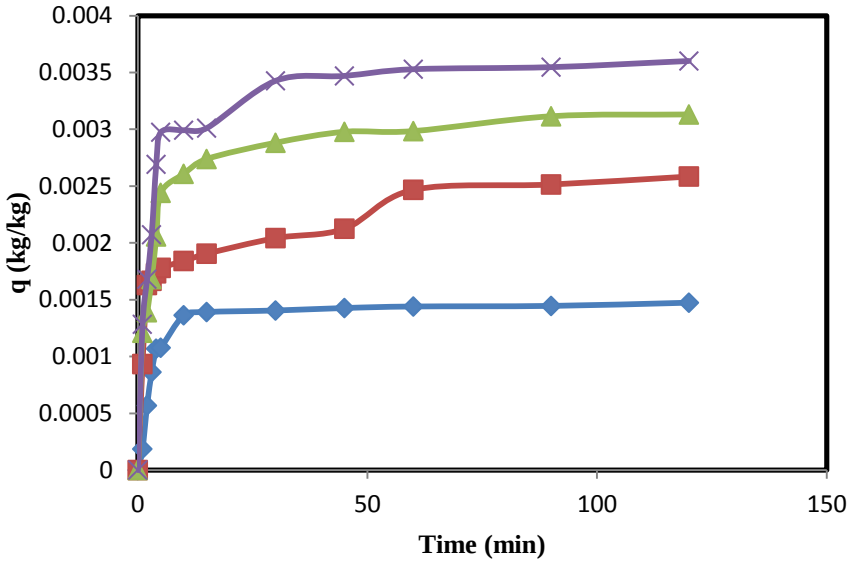

Figure 4.6 Effect of contact time on adsorption of Mn^{2+} with initial pH of 7 and 1 g of MOCZ for◆ 50 mg/L,■ 100mg/L, ▲ 150 mg/L and X 200 mg/L

4.2.3 Effect of MOCZ dosage

The relationship between the amounts of Mn^{2+} adsorbed by MOCZ with the adsorbent dosage was shown in Appendix B3 and Figure 4.7. From the graph, the amount of Mn^{2+} adsorbed by MOCZ increased when increased the adsorbent dosage from 0.5g, 0.7g and 1g.

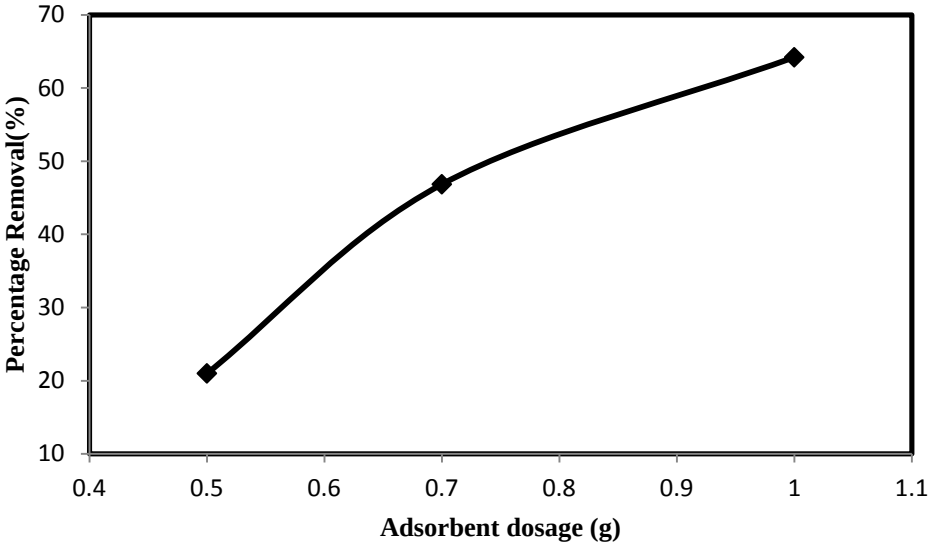

Figure 4.7 Effect of adsorbent dosage on removal of Mn^{2+} with initial concentration of 150 mg/L at pH 7

The data was used to derive a mathematical relationship to relate the Mn^{2+} removal to adsorbent dosage. The empirical relation for removal was shown in equation (2) and simplified becomes equation (3) (Mozumder, et al., 2008)

$$\frac{1}{R} = \frac{n'}{m_a} + M \tag{2}$$

$$R = \frac{m_a}{n' + m_a M} \tag{3}$$

where R and m_a are the percentage removal (%) and amount of adsorbent dosage (g) and $n'$and M are the constant.

By plotting $\frac{1}{R}$ versus$\frac{1}{m_a}$, we can find a straight line which was shown in Figure 4.8 and the data was tabulated in Appendix B4.

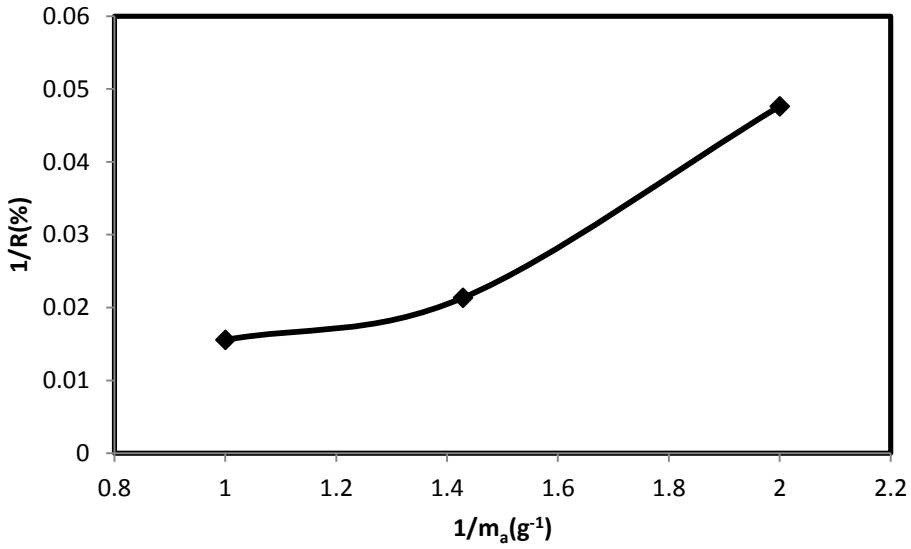

Figure 4.8 Empirical relation for adsorbent dosage with % removal

From Figure 4.8, we get M = 0.0202 and n'=0.00328. Therefore, we can establish an empirical relation between percentage removal and adsorbent dosage by substitute the constant value into equation 3

$$R = \frac{m_a}{0.00328 + 0.0202 m_a} \quad (4)$$

4.2.4 Effect of initial pH

As shown in the Figure 4.9, the Mn^{2+} ions adsorption by MOCZ enhanced with the increase of medium pH from 4 to 8 by using Mn^{2+} aqueous solution at 150mg/L. At lower pH values, Mn^{2+} ions removal was inhibited possibly as a result of a competition between H^{+} and Mn^{2+} on surface exchangeable sites with an

apparent preponderance of H+ ions. As the pH increased, the negative charge density on MOCZ surface increases due to deprotonation of the metal binding sites and thus the Mn^{2+} ions adsorption increased. Table 4.2 showed the initial pH and final pH after adsorption of Mn^{2+} by MOCZ.

Table 4.2 pH changes after adsorption of Mn^{2+}

Initial pH	Final pH
4	3.8
5	4.6
6	5.5
7	5.86
8	6.09

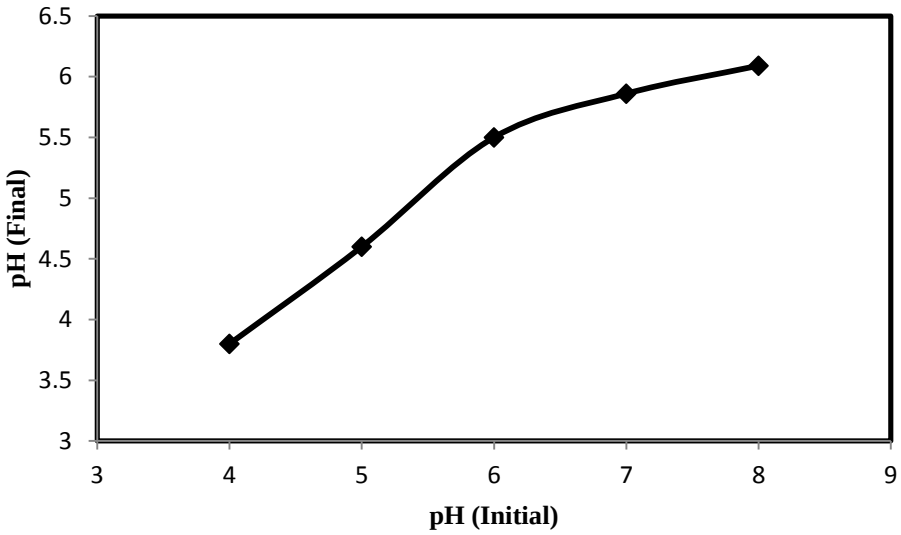

Figure 4.9 pH changes after adsorption of Mn^{2+} at initial concentration 150 mg/L with 1g of adsorbent

In order to understand the adsorption mechanism, the variation of solution pH during adsorption was measured, and the results were shown in Figure 4.9. The pH values at the end of experiments decreased after adsorption by MOCZ. These results indicated that mechanisms by means of which Mn^{2+} ions were adsorbed onto MOCZ

involved an ion exchange reaction of Mn^{2+} with H^{+} on the surface and also a surface complex formation.

Table 4.3 Chemical reaction equation for manganese species (Junior et al., 2010)

Reaction	Equilibrium constant	Reference
$Mn^{2+} + SO_4^{2-} = MnSO_4$	$K_1 = 190$	Bjerrum et al. (1958)
$Mn^{2+} + HSO_4^{-} = MnHSO_4^{+}$	$K_2 = 181.97$	Smith and Martell (1982)
$Mn^{2+} + OH^{-} = MnOH^{+}$	$K_3 = 6.27 \times 10^3$	Shock et al. (1997)
$Mn^{2+} + 2OH^{-} = Mn(OH)_2$	$K_4 = 6.31 \times 10^{12}$	Landolt-Bornstein (1999)

The value of K for each reaction can be expressed in terms of Mn^{2+} concentration where

$$K_1 = \frac{[MnSO_4]}{[Mn^{2+}][SO_4^{2-}]} \quad (5)$$

$$K_2 = \frac{[MnHSO_4^{+}]}{[Mn^{2+}][HSO_4^{2-}]} \quad (6)$$

$$K_3 = \frac{[MnOH^{+}]}{[Mn^{2+}][OH^{-}]} \quad (7)$$

$$K_4 = \frac{[Mn(OH)_2]}{[Mn^{2+}][OH^{-}]^2} \quad (8)$$

By using Equation 5 until 8, concentration of different manganese ion was calculated using the equilibrium constant in Table 4.3 and graph relative concentration C_i/C_T against pH was plotted in Figure 4.10. Details calculations were shown in Appendix B5.

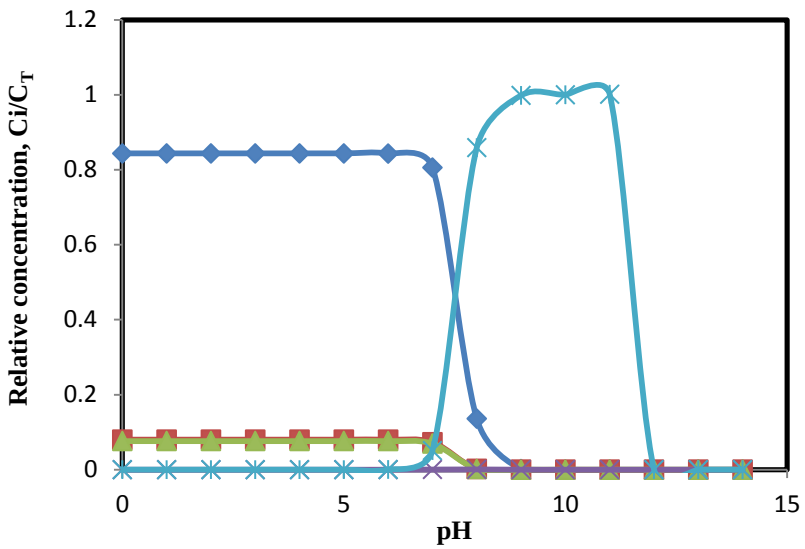

Figure 4.10 Relative concentration of different manganese species at different pH at Mn^{2+} concentration of 0.00592mol/L with 1g of MOCZ for ◆ Mn^{2+}, ■ $MnSO_4$, ▲ $MnHSO_4$, X $MnOH^+$, ✳ $Mn(OH)_2$

At low pH, the Mn species adsorbed on MOCZ are predominantly Mn^{2+} ions as shown in Figure 1 and the adsorption occur mainly by ion-exchange. This can be seen by final pH variation (Figure 4.10) that remains practically constant until pH 6.0 and in this case for each Mn^{2+} ions adsorbed is released one H^+ ion.

As the medium pH increase, the formation of hydrolysis complex ($Mn(OH)^+$) increase and the manganese species adsorbed are mainly in a complex form. In this case for each Mn^{2+} ion adsorbed, two H^+ ions are released. Figure 4.10 showed that for a pH higher than 6, the pH variation in final pH is greater and the Mn^{2+} and $Mn(OH)^+$ concentrations adsorbed will be approaching, thus $[\equiv MnOMn^+]$ and $[\equiv MnOMnOH]$become approximately equal.

The surface reaction of divalent ions with oxide surfaces has been described by a number of different authors (Hohl and Stumn, 1976; Benjamin and Leckie, 1981; Fu et al., 1991; Han et al., 2006). Main interactions are summarized as:

(1) Association of the free metal ion with a surface hydroxyl group (ion exchange with H^+ ion),

$$\equiv MnOH + X^{2+} \leftrightarrow MnOX^+ + H^+ \quad (9)$$

(2) Adsorption and formation of a hydrolysis complex,

$$\equiv MnOH + X^{2+} + H_2O \leftrightarrow MnOXOH + 2H^+ \quad (10)$$

(3) Formation of a bidendate complex

$$2(\equiv MnOH) + X^{2+} \leftrightarrow (\equiv MnO)_2X + 2H^+ \quad (11)$$

According to these reactions mechanisms, the more Mn^{2+} ions are adsorbed onto MOCZ, the more hydrogen ions are released the lower the medium pH. The release of one H^+ ion for each Mn^{2+} ions adsorbed would suggest the ion-exchange with the surface whereas the release of two H^+ ions for each Mn^{2+} ions adsorbed would suggest either the formation of hydrolysis complex or a bidendate complex which was shown in Figure 4.9.

4.3 Adsorption isotherms

The equilibrium data, commonly known as adsorption isotherms are basic parameters for the design of adsorption systems (Perry and Green, 1999) and these data provide information on the adsorbent capacity or the amount required to remove a pollutant mass under the system conditions. The Langmuir and modified Langmuir models' equations are commonly used to describe the adsorption isotherms at constant temperature for application in the water and wastewater model treatment design.

The Langmuir adsorption isotherm is valid for monolayer adsorption onto a surface containing a finite number of ideal sites. This model assumes uniform energies of adsorption onto the surface and no transmigration of adsorbate in the plane of the surface. The Langmuir adsorption isotherm for solid-liquid adsorption system can be represented by the following equation 12

$$q = \frac{q_{max} K C_f}{1 + K C_f} \tag{12}$$

where Langmuir parameters q_{max} (kg Mn^{2+} kg^{-1}) and K (m^3 $kg^{-1}Mn^{2+}$) of equation 12 are the maximum capacity adsorption at high equilibrium concentrations (attaining adsorbent monolayer) and the equilibrium constant, respectively (Perry and Green, 1999). Langmuir data fitting were done by linearization of equation 12, given by equation 13

$$\frac{1}{q} = \frac{1}{Kq_{max}}\frac{1}{C_f} + \frac{1}{q_{max}} \quad (13)$$

The Mn^{2+} uptake (q), expressed as Mn^{2+} removal per unit mass of adsorbent (kg Mn^{2+} kg^{-1}) was calculated using equation 14

$$q = \frac{(C_o - C_f)V}{m} \quad (14)$$

where q is the amount of metal ions adsorbed on the MOCZ, C_o and C_f are the concentration of metal ions in the solution (kg Mn^{2+} m^{-3}) prior to and after adsorption, V is the volume of the aqueous phase (m^3), and m is the dry weight of the adsorbent (kg). Graph $1/q$ against $1/C_e$ was plotted as in Figure 4.11 and the corresponding data were shown in the Appendix B6.

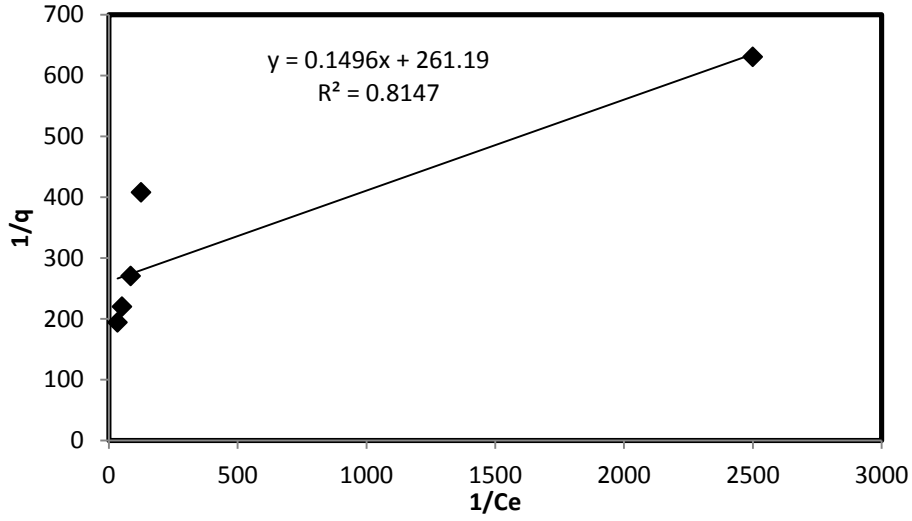

Figure 4.11 Langmuir Isotherm Curve

The essential characteristics of Langmuir isotherm can be expressed by a dimensional constant called equilibrium parameter, R_L that is defined by

$$R_L = \frac{1}{1 + KC_o} \quad (15)$$

where K is the Langmuir constant (m^3/kg) that indicates the nature of adsorption and Co is the initial Mn^{2+} concentration in mg/L. The value of R_L indicates the type of the adsorption isotherm as in Table 4.4.

Table 4.4 R_L value and isotherm

R_L value	Types of Isotherm
$R_L>1$	Unfavorable
$R_L=1$	Linear
$0<R_L<1$	Favorable
$R_L=0$	Irreversible

Based on equation 15, R_L value was 0.00009 indicates that the type of behavior of Mn^{2+} adsorption was favorable.

4.4 Adsorption kinetics

Kinetic models have been used in order to investigate the controlling mechanism of adsorption processes such as mass transfer and chemical reaction. The pseudo-first order and pseudo-second order equations are applied to model the kinetics of Mn^{2+} heavy metals adsorption onto manganese oxide coated zeolite. The pseudo-first order equation was shown in Equation 16 reported by Lagergren (1989)

$$\log(q_e - q_t) = \log(q_e) - \frac{k_1}{2303} t \quad (16)$$

where q_e is the amount of heavy metal ion adsorbed at equilibrium (kg/kg), q_t is the amount adsorbed at time t (kg/kg), $k_1$is the Lagergren pseudo-first order adsorption rate constant (min^{-1}). A linear graph of $\log(q_e - q_t)$ against t was plotted to retain the value of k_1 from the slope of the Figure 4.12. The corresponding data were shown in the Appendix B7.

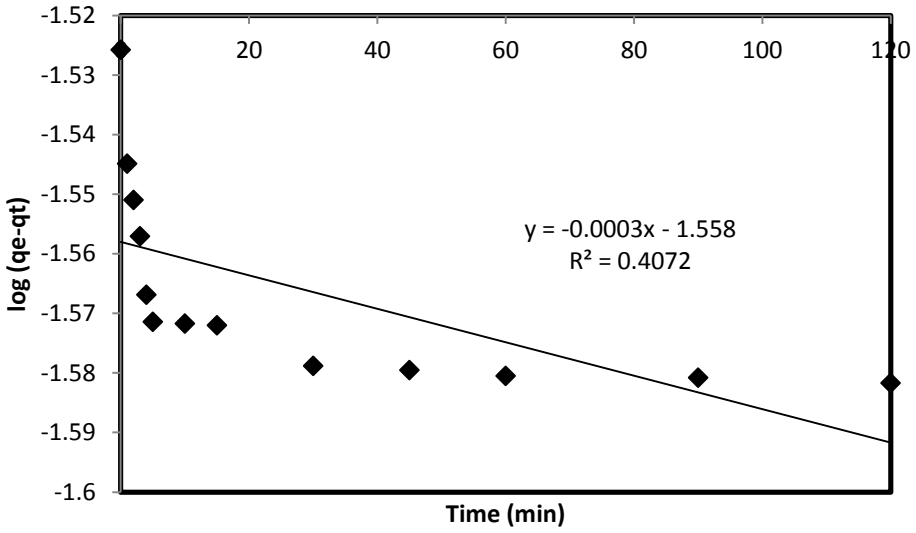

Figure 4.12 Pseudo-first order kinetic for adsorption of Mn^{2+} by MOCZ (Concentration at 200mg/L with initial pH 7.4)

The pseudo-second order equation is expressed as in equation 17

$$\frac{t}{q_t} = \frac{1}{k_2 q_e^2} + \frac{1}{q_e} t \quad (17)$$

where k_2 is the second order adsorption rate constant (kg $kg^{-1}min^{-1}$). Graph t/q_t against t was plotted and it should give a straight line if pseudo-second order kinetics is applicable. And for q_e and k_2 can be determined from the slope and intercept of the plot from the graph. The plots of linearized form of the pseudo-second order adsorption kinetic are shown in Figure 4.13.

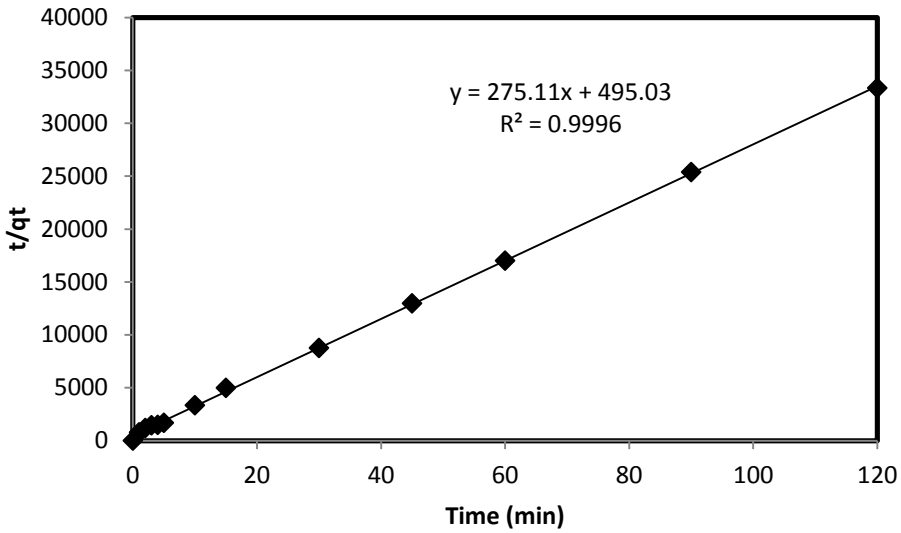

Figure 4.13 Pseudo second order kinetic for adsorption of Mn^{2+} by MOCZ (Concentration at 200mg/L with initial pH 7.4)

The pseudo-first order and pseudo-second order rate constant and corresponding coefficient for adsorption of MOCZ are summarized in Table 4.5. From the calculated values below, the adsorption of Mn^{2+} by MOCZ are more favorable towards pseudo-second order kinetics due to higher value of R^2 and in the range of 0 to 1.

Table 4.5 Kinetic constants of Mn^{2+} ions adsorption onto MOCZ

Adsorbent	q_e(exp)	Pseudo-first order model			Pseudo-second order model		
		k_1 (min^{-1})	q_e(theor.) (meq g^{-1})	R^2	k_2	q_e(theor) (meq g^{-1})	R^2
MOCZ	0.0298	0.6909	33.99	0.407	152.89	0.0036	0.999

If the adsorption process is described by Langmuir model, it is logical that the adsorption rate $dq\ /\ dt$ should be

$$\frac{dq}{dt} = k_1\ (q_\infty - q)C_B - k_2\ q \tag{18}$$

where q is the amount of Mn^{2+} adsorbed (kg/kg) at time t, C_B is the bulk concentration of Mn^{2+} (kg/m^3) at time t.

Solving Equation 18, we obtain the relation $q\ vs\ t$

$$\frac{1}{\alpha(\alpha-\beta)}\ln\frac{(q-\alpha)\beta}{(q-\beta)\alpha} = k_1 t \tag{19}$$

$$q = (\alpha-\beta)\frac{(\frac{\beta}{\alpha})e^{(\beta-\alpha)ak_1t}}{\left(\frac{\beta}{\alpha}\right)e^{(\beta-\alpha)ak_1t}-1} + \beta \tag{20}$$

With

$$\alpha = \frac{b+\sqrt{b^2-4ca}}{2a} \tag{21}$$

$$\beta = \frac{b-\sqrt{b^2-4ca}}{2a} \tag{22}$$

Where

$$a = w_a \tag{23}$$

$$b = C_o + w_a q_\infty + \frac{1}{K} \tag{24}$$

$$c = q_\infty C_o \tag{25}$$

For $t \to \infty$, $q = q_e = \beta$. Therefore, the calculated value of β directly gives the equilibrium batch adsorption density for a given initial concentration C_o and adsorbent dosage w_a. Experimental value and theoretical value for Langmuir model was calculated and the corresponding data was plotted in Figure 4.14 and in Appendix B8. The value of k_1 and k_2 are calculated and summarized in the Table 4.6.

Table 4.6 Kinetic constant of Mn^{2+} for Langmuir model

Initial Concentration (mg/L)	K	k_1	k_2	R^2
50	214.96	461 ± 39	5.06 ± 1	0.2791

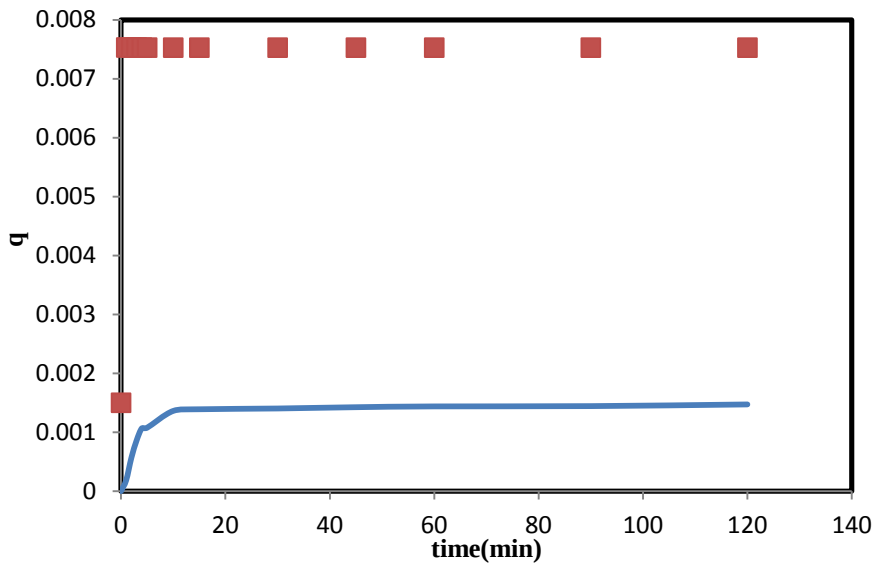

Figure 4.14 Theoretical and experimental amount of adsorbed Mn^{2+} at 50mg/L with 1g of MOCZ for —— q experiment, ■ q theoretical

It can be concluded that the experimental data did not fixed well with the Langmuir model as the initial rate of adsorption is too high. Therefore, two sites one molecule mechanism have been studied. In this mechanism, one molecule will occupy two sites of adsorbent.

4.4.1 Modification of Langmuir model

In two sites one molecule type of adsorption, the reaction equation become (Mozammel et al., 2010)

$$B + 2S \overset{K}{\Leftrightarrow} S_2B \tag{26}$$

$$K = \frac{k_1}{k_2} = \frac{C_{S_2B}}{C_B C_B^2} \tag{27}$$

According to this adsorption phenomenon, it is required two sites to fit one molecule. So, the number of active site is double to the number of adsorbate molecules adsorbed. Thus,

$$C_{S_o} = \frac{2q_\infty w}{v} \tag{28}$$

$$C_{S_2B} = \frac{2qw}{v} \tag{29}$$

$$K = \frac{C_{S_2B}}{C_B(C_{S_o} - C_{S_2B})^2} \tag{30}$$

$$KC_B = \frac{w}{2v}\frac{q}{(q_\infty - q)^2} \tag{31}$$

The rate of changes of occupied sites

$$\frac{dC_{S_2B}}{dt} = k_1 C_B C_S^2 - k_2 C_{S_2B} \tag{32}$$

$$C_s = C_{S_o} - C_{S_2B} \tag{33}$$

Therefore, the kinetic model for two sites one molecules is shown as below:

$$\frac{dq}{dt} = k_1 C_B \frac{2w}{v}(q_\infty - q)^2 - k_2 q \tag{34}$$

The equilibrium data are fitted using the equations below:

$$q = q_\infty - \sqrt{\frac{w}{2Kv}}\sqrt{\frac{q}{C_B}} \tag{35}$$

Graph q versus $\sqrt{\frac{q}{C_B}}$ are plotted in Figure 4.15, then q_∞ can be calculated from the intercept and K can be calculated from the slope. Corresponding data was in Appendix B9.

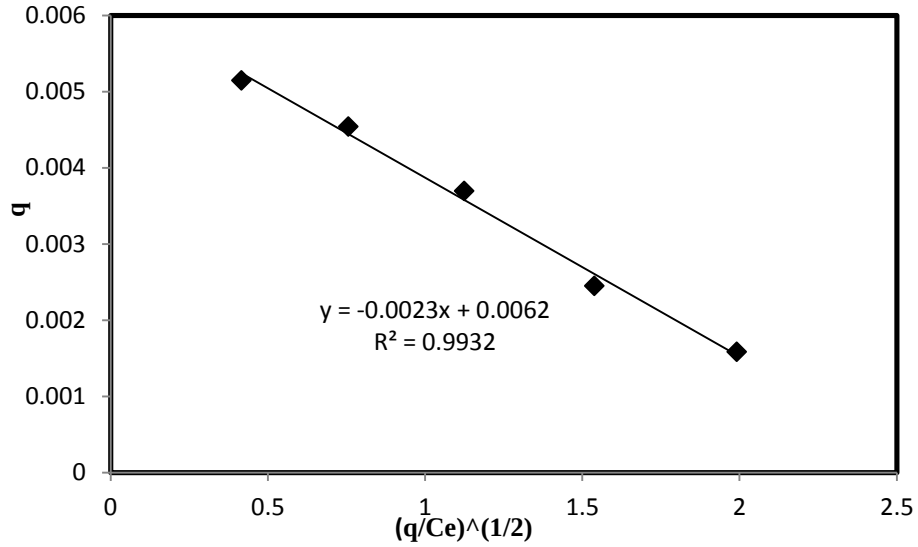

Figure 4.15 Two sites one molecule isotherm curve

Kinetic parameters k_1 and k_2 are determined by using initial rate method (Fogler, 2002). It is assumed that when time $\rightarrow 0$, $q \ll q_\infty$ and is constant for all initial concentration q_i for a given system. Then Equation 32 becomes

$$\frac{dq}{dt} = k_1 q_\infty \frac{2w}{v} C_B - k_2 q_i \tag{36}$$

For different initial concentration, the initial adsorption rate dq/dt are measured and dq/dt versus C_{BO} was plotted. Corresponding data was in Appendix B10. As k_2 is constant and qi is constant for a system with a definite mechanism, so k_1 can be calculated from slope of the straight lines. k_2 can be calculated from the relation $k_2 = k_1/K$. The value of k_1 and k_2 were used to calculate the theoretical value of dq/dt and this value was plotted against time t. Resulted curves are compared with the experimental one.

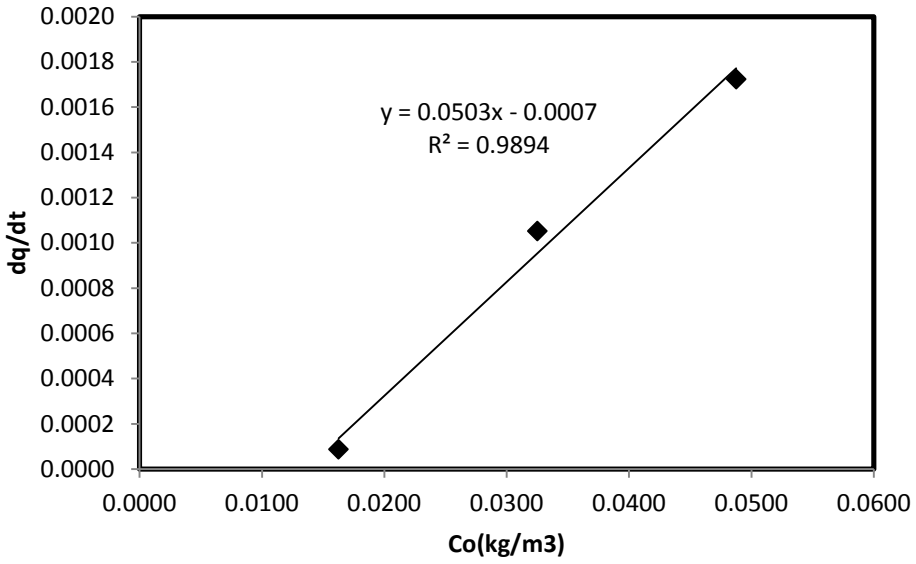

Figure 4.16 Plot for determination of k_1 for the system

From the graph, we get the value of $k_1 = 0.002714$ and $k_2 = 1.3875 \times 10^{-6}$.

Table 4.7 Equilibrium and kinetic adsorption parameters, R^2 values for different system considering different mechanism

System	Mechanism	Equilibrium			Kinetic	
		K	q_{max}	R^2	k_1	k_2
MOCZ	Langmuir	214.96	0.00693	0.82	461 ± 39	5.064 ± 1
	Two sites one molecule	1955.97	0.9267	0.99	0.0027	1.39×10^{-6}

Using the values of k_1 and k_2, the theoretical values of dq/dt for Langmuir and two sites one molecule mechanisms are calculated. These calculated values are plotted against the corresponding time t, and the resulted curves were compared with the experimental dq/dt against t curve. The values of experimental and theoretical dq/dt values were shown in the Appendix B11 Figure 4.17 to Figure 4.20 showed the comparison between the experimental and theoretical value by considering two site one molecule mechanism and Langmuir model.

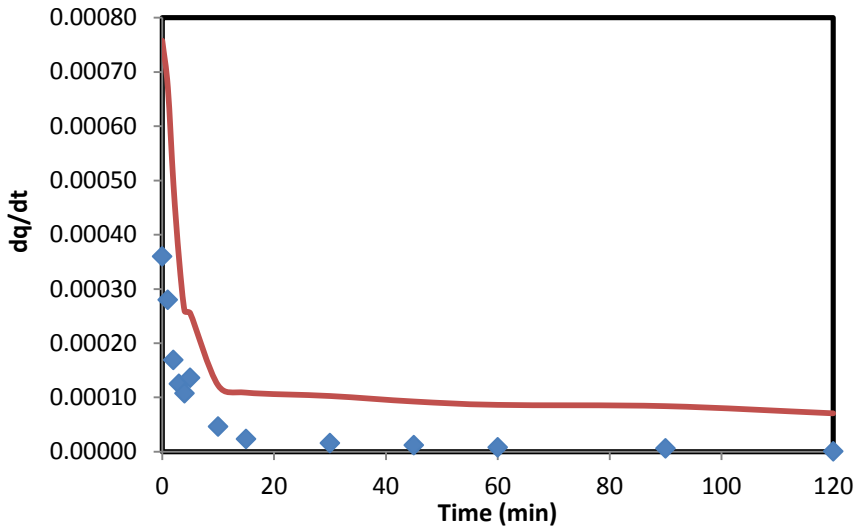

(a)

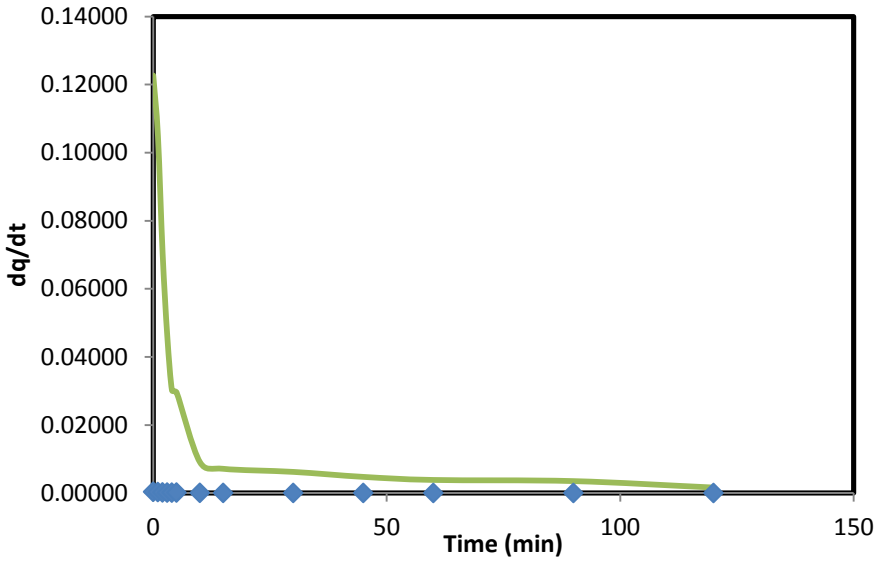

(b)

Figure 4.17 The experimental and theoretical by considering different mechanism at initial concentration 50 mg/L with 1g of MOCZ (a) two sites one molecule (b) Langmuir for ◆ experimental, — Two sites one molecule, — Langmuir

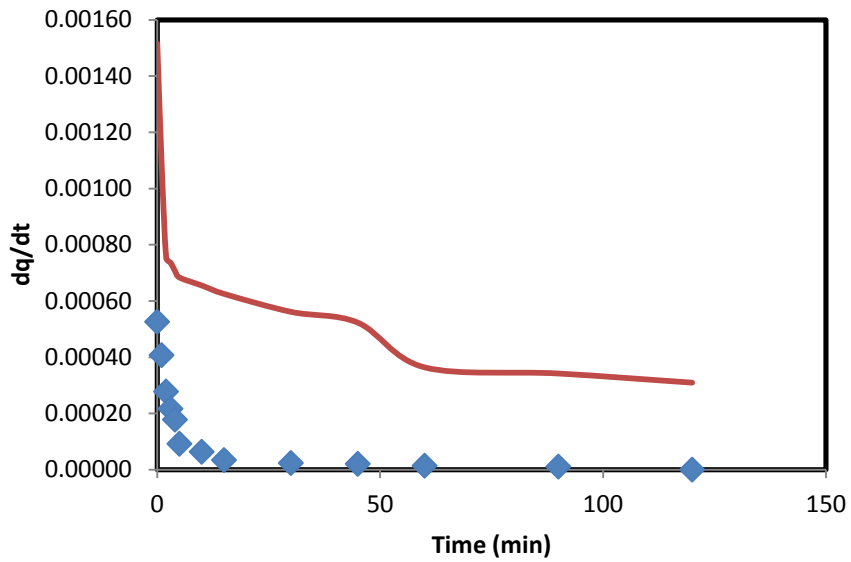

(a)

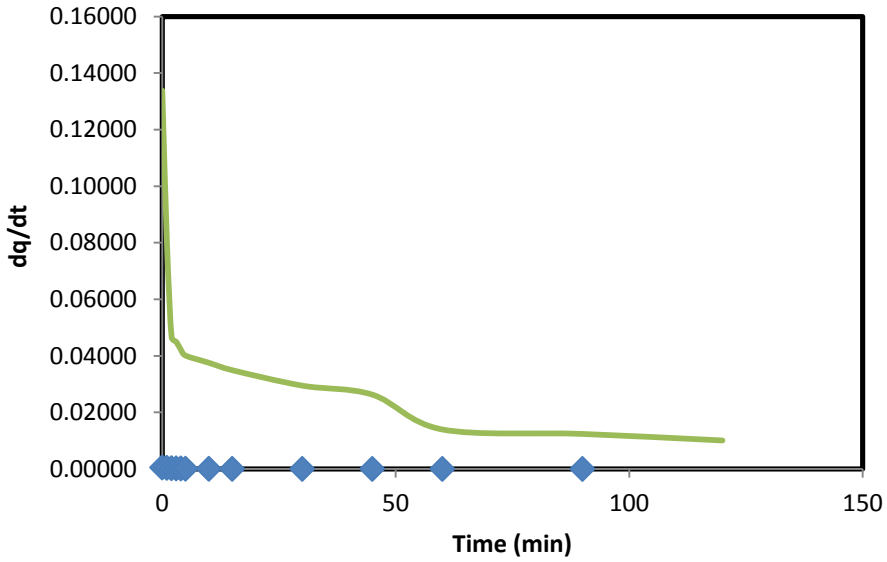

(b)

Figure 4.18 The experimental and theoretical by considering different mechanism at initial concentration 100 mg/L with 1 g of MOCZ (a) two sites one molecule (b) Langmuir for ◆ experimental, — two sites one molecule, — Langmuir

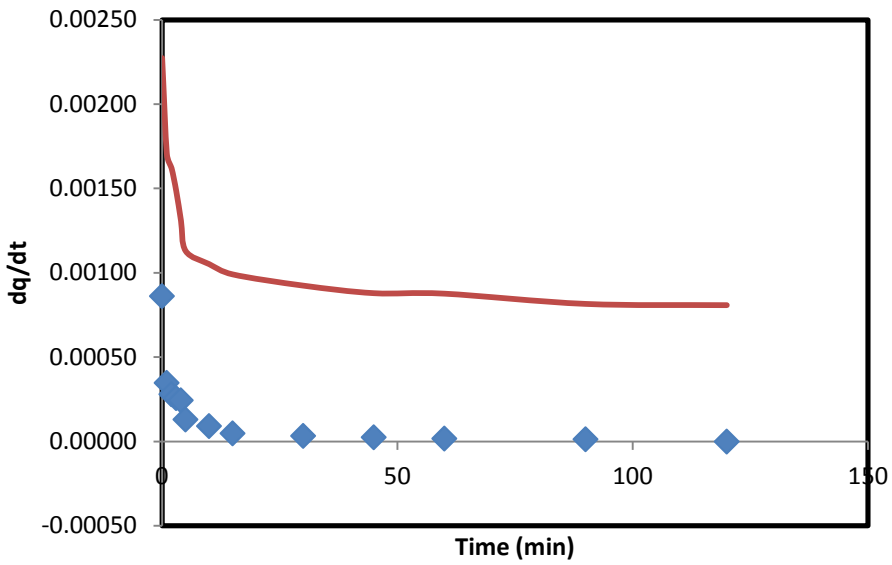

(a)

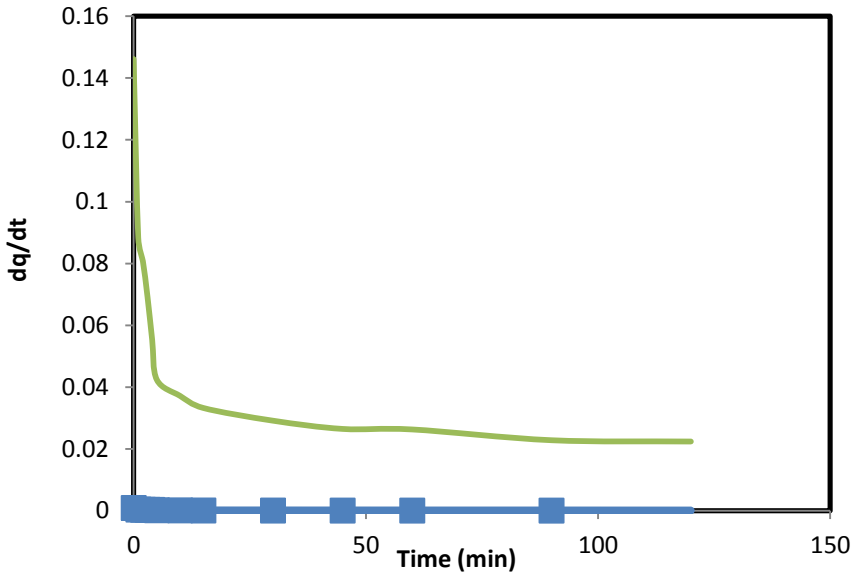

(b)

Figure 4.19 The experimental and theoretical by considering different mechanism at initial concentration 150 mg/L with 1 g of MOCZ (a) two sites one molecule (b) Langmuir for ◆ experimental, — two sites one molecule, — Langmuir

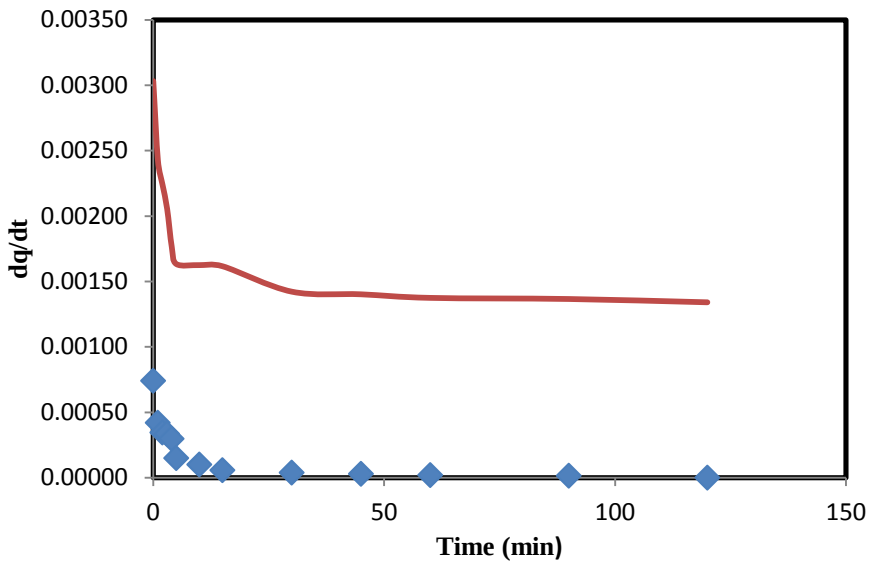

(a)

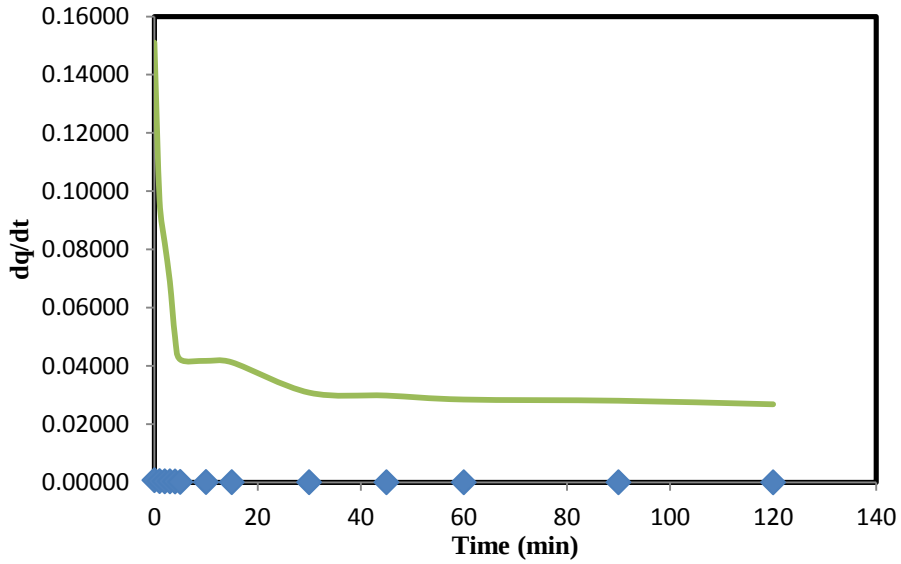

(b)

Figure 4.20 The experimental and theoretical by considering different mechanism at initial concentration 200 mg/L with 1 g of MOCZ (a) two sites one molecule (b) Langmuir for ◆ experimental, — two sites one molecule, — Langmuir

In the adsorption of Mn^{2+} by MOCZ, the two mechanisms which is the Langmuir models and two sites one molecule system are applicable and the curves for the system at 50mg/L to 200 mg/L initial concentration were presented in Figure 4.17 to Figure 4.20. It can be seen that the data did not fixed well with the Langmuir model. But the modified Langmuir model, which is the two sites one molecule model, satisfied the data well. It can be concluded that the adsorption of Mn^{2+} using MOCZ followed the two sites one molecule mechanism where one molecule will occupy two sites of adsorbent.

Resulted curve were compared with the experimental and the values of standard deviations were calculated (Cristian, 1994) and the data were shown in the Table 4.8. It can be concluded that due to the smaller value of standard deviation, two sites one molecule mechanism is the most applicable mechanism for this system.

Table 4.8 Standard deviation value for Langmuir and Two sites one molecule mechanism

Initial concentration (mg/L)	Standard deviation	
	Langmuir model	Two sites one molecule
50	0.03372	0.0001
100	0.03283	0.0002
150	0.03576	0.0002
200	0.03622	0.0003

CHAPTER 5

CONCLUSION AND RECOMMENDATION

5.1 Conclusion

The MOCZ (manganese oxide coated zeolite) had low crystallinity degree, and the oxide coated on zeolite surface is presented mainly as vernadite (δMnO2) with specific surface area of 39.9 m^2g^{-1} and average pore size diameter of 1.1733 nm. The coating is composed of attached small particles on the zeolite surface.

Results showed that the amount of Mn^{2+} adsorbed increase with pH and adsorbent dose that the adsorption kinetics study of the Mn^{2+} followed a pseudo-second-order model. This indicates that the adsorption may be controlled by chemical adsorption. Furthermore, the modified Langmuir model which is the two sites one molecule model fitted well equilibrium data, showing a strong adsorption capacity for Mn^{2+} ions reaching a maximum capacity of 0.9267 meq $Mn^{2+}g^{-1}$. Mn^{2+} ions uptake is the result as a combination of several interfacial reactions namely, ion

exchange, chemisorptions and adsorption as potential determining ions. Results found showed that the modified zeolite shows a good potential as adsorbent for Mn^{2+} ions.

5.2 Recommendations

Some recommendations have been made to improve the result for future work.

i. Coating the zeolite with different amount of potassium permanganate in order to study the effect of manganese loading rate to the adsorption study
ii. Using low concentration of $MnSO_4.H_2O$ solution for kinetic study, for example 5 mg/L, 10 mg/L and 15 mg/L
iii. Using different manganese salt to prepare sythetic wastewater
iv. Using manganese oxide coated zeolite in removal others heavy metals

REFERENCES

Agency for toxic substances and disease registry, national center for environmental health (2008). Public Health Statement of manganese. The encyclopedia of earth. April 1, 2008.

Alyuz, B. & Veli, S. (2009). Kinetics and equilibrium studies for the removal of nickel and zinc from aqueous solutions by ion exchange resins. Journal of Hazardous materials 167, pg 482- 488

Babel, S. & Kurniawan, T. A. (2003). Low cost adsorbents for heavy metals uptake from contaminated water: A review. Journal of Hazardous Materials B97, 219-243

Balistrieri, L.S., Murray, J.W. (1982). The surface chemistry of dMnO2 in major ionseawater. Geochimica et Cosmochimica Acta 46, pg 1041–1052.

Barakat, M. A. (2010). New trends in removing heavy metals from industrial wastewater. Arabian Journal of Chemistry, 4, pg 361-377

Benjamin, M.M., Leckie, J.O. (1981). Multiple-site adsorption of Cd, Cu, Zn, and Pb on amorphous iron oxyhydroxide. Journal of Colloid and Interface Science 79 (1), pg 209–221.

Bjerrum, J., Schwarzenbach, G., Sillen, L. G. (1958). Stability Constants of metal ion complexes, Part II, Scpcial Publ. 7. The chemical society, London, UK, pg 131.

Chang, I. & Kim, S. (2005). Wastewater treatment using membrane filtration- Effect of biosolids concentration on cake resistance. Process Biochemistry 40

Ceribasi, I. H. & Yetis, U. (2001). Bisorption of Ni(II) and Pb(II) by Phanerochaete chrysosprium from a binary metal system – Kinetics. Water S. A. Volume 27

Cristian, G. D. (1994). Analytical Chemistry. Fifth edition, John Wiley & Sons. New York.

Environmental Fact Sheet (2006). Manganese: Health Information Summary. New Hampshire department of environmental services.

Fogler, H. S. (2002). Elements of Chemical Reaction Engineering. Third Edition, Prentice – Hall : New Delhi

Fu, F. & Wang, Q. (2011). Removal of heavy metal ions from wastewaters. A review. Journal of Environmental Manangement 92, 2011, pg 407-418

Fu, G., Allen, H.E. & Cowan, C.E. (1991). Adsorption of cadmium and copper by manganese oxide. Soil Science 152, pg 72–81.

Grandt, A. F. & Mcdonald, D. G. (1981). Limestone-Lime treatment of Acid Mine Drainage-Full Scale-Project Summary. Environmental Protection Agency Office of Research and Development, 81 (33) 600/S7

Geankoplis, C. J. (2003). Transport Processes and Separation Process Principles (Includes Unit Operations) 4th edition. Pearson : USA

Gupta, V. K. & Suhas. (2009). Application of low cost adsorbents for dye removal-A review. Journal of Environmental Manangement 90, pg 2313-2342

Han, R., Zou, W., Zhang, Z., Shi, J., Yang, J. (2006). Removal of copper(II) and lead(II) from aqueous solution by manganese oxide coated sand I. Characterization and kinetic study. Journal of Hazardous Materials B 137, pg 384–395.

Helmer, R. & Hespanhol, I. (1997). Water pollution control- A guide to use water quality manangement principeles. United Nations Environment Progamme, Water supply and Sanitation Collaborative Council, World health organization, ISBN 0419 229108

Hohl, H., Stumm, W. (1976). Interaction of Pb^{2+} with hydrous c-AI2O3. Journal of Colloid and Interface Science 55 (2), pg 281–288.

Iwa water wiki. (2010). Removal technologies in wastewater treatment.

Kampa, M. & Castanas, E. (2008). Human health effects of air pollution. Environmental Pollution. Proceedings of the 4th International Workshop on biomonitoring of atmospheric Pollution (with emphasis on trace elements). Volume 151, issue 2, January 2008, pg 362-367

Kang S.Y., Lee J.U., Moon S.H. and Kim K.W. (2004). Competitive adsorption characteristics of Co2þ, Ni2þ and Cr3þ by IRN-77 cation exchange resin in synthesized wastewater, Chemosphere, 56, pg 141-147

Tiller, K. Y. (1989). Heavy metals in soil and their environmental significance, Advanced soil science, 9, pg 113-142

Lagergren, S. (1989). Zur Theorie der sogenannten adsorption gelöster stoff Kungliga Svenska Vetenskapasakademiens Handlingar 24(4), pg 1–39.

Landolt-Bornstein (1999). Thermodynamics equilibria of the extraction of cobalt(II) from Scientific Group Thermodata Europe (SGTE). Springer Verlag, Berlin-Heidelberg, Germany, pg 405

Manganese. Air quality guidelines. WHO Regional Office for Europe, Copenhagen, Denmark, 2001.

Mozammel, T., Khan, M. R. & Islam, M. A. (2010). Dye Absorption in batch mode: equilibrium and kinetic modeling. Proceedings of the Conference on Engineering Research, Innovation and Education 2010.

Mozumder, S. I.. Khan, M. R., Islam, M. A. (2008). Kinetics and mechanism of Cr(VI) adsorption onto tea-leaves waste. Asia Pacific Journal of Chemical Engineering. Volume 3, Issue 4, pg 452-458.

Malaysia Sewage and Industrial Effluent Discharge Standards (n.d.).

Mohan, D. & Singh, K. (2002). Single and multi component adsorption of cadmium and zinc using activated carbon derived from bagasse – an agriculture waste. Water Research, 36, pg 2304-2318

Monser, L. & Adhoum, N. (2001). Modified activated carbon for the removal of copper, zinc, chromium and cyanide from wastewater. Journal of separation and Purification Technology, 26, 137-146

Mengistie, A. A., Rao, T.S. & Rao, A. V. P. (2012). Adsorption of Mn(II) ions from wastewater using activated carbon obtained from birbira (Militia Ferruginea) leaves. Global Journal of Science Frontier research

Ng, K. C., Chua, H. T., Chung, C.Y., Loke, C. H., Kashiwagi, T., Akisawa, A. & Saha, B. B. (2001). Experimental investigation of the silica gel- water adsorption isotherm characteristics. Applied Thermal Engineering. Volume 21, Issue 16, pg 1631-1642.

Peavy, H. S., Rowe, D. R. & Tchnobangoglous, G. (1985). Environmental Engineering International Edition. McGraw Hill Book : SingaporePehlivan, E. & Altun, T. (2006). Ion-exchange of Pb^{2+}, Cu^{2+}, Zn^{2+}, Cd^{2+}, and Ni^{2+} ions from aqueous solution by Lewatit CNP 80. Journal of Hazardous materials. Volume 140, Issues 1-2, pg 299-307

Perry, R., Green, D. (1999). Perry's Chemical Engineers' Handbook, Seventh Edition. McGraw-Hill, New York, USA.

Ritchter, M., Berndt, H., Eckelt, R., Schneider, M., Fricke, R. (1999). Zeolite-mediated removal of NOx by NH_3 from exhaust streams at low temperatures. Catalysis Today, 54, pg 531-545.

Sayed, G. O., Dessouki, H. A., and Ibrahiem, S. S. (2011). Removal of Zn (II), Cd(II) and Mn(II) from aqueous solutions by adsorption on maize stalks. The Malaysian Journal of Analytical Sciences, Vol 15, No.1, pg 8-21

Sharma, D. C. and Forster, C. F. (1994). A preliminary examination into the adsorption of hexavalent chromium using low cost adsorbents. Biores. Technology, 47, pg 257-264

Salam, O. E. A., Reiad, N. A. & Elshafei, M. M. (2011). A study of the removal characteristics of heavy metals from wastewater by low –cost adsorbents. Journal of Advanced Research 2011, 2, pg 297-303

Smith, R. M., Martell, A. F. (1982). Critically Stability Constants, Vol 5. Plenum Press, pg79-84

Shock, E. L., Sassani, D. C., Wills, M., Sverjensky, D. A. (1997). Inorganic species in geological fluids: correlations among standard molal thermodynamic properties of aqueous ion and hydroxide complexes. Geochim. Cosmochim. Acta 61, pg 907-950.

Singare, P. U., Mishra, R. M. & Trivedi, M. P. (2012). Sediment Contamination Due to Toxic Heavy Metals in Mithi River of Mumbai. Advances in Analytical Chemistry. 2(3):14-24.

Southichak, B., Nakano, K., Normura, M., Chibia, N. and Nishmura, O. (2006). "Pharagmites australis: a novel bio-adsorbent for the removal of heavy metals from aqueous solution", Water Res., 2006, 40, pg 2295-2302.

Taffarel, S. R., Rubio, J. (2008). On the removal of Mn^{2+} ions by adsorption onto natural and activated Chilean zeolites. Minerals Engineering 22 (4), pg 336-343

Taffarel, S. R., Rubio, J. (2010). Removal of Mn^{2+} from aqueous solution by manganese oxide coated zeolite. Minerals Engineering 23, pg 1131-1138

Teng, S. X., Wang, S. G., Gong, W. X., Liu, X. W., Gao, B. Y. (2009). Removal of fluoride by hydrous manganese oxide coated alumina: performance and mechanism. Journal of Hazardous materials 1168, 2-3, pg 1004-1011

APPENDIX A Photos During Experiment

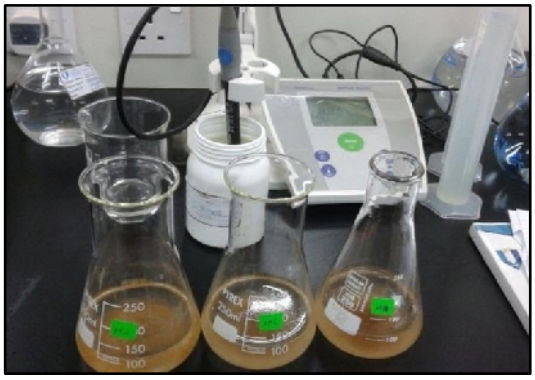

Appendix A1 pH adjustment

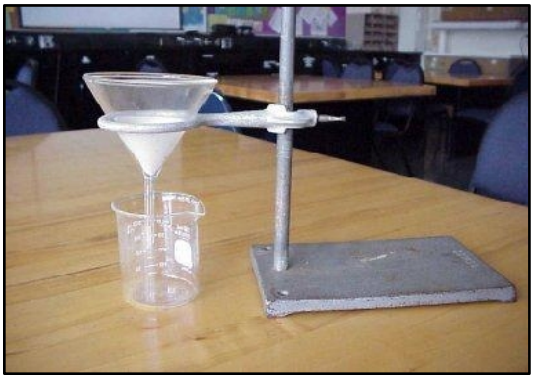

Appendix A4 Samples were filtered by using filter paper

Appendix A2 Samples were agitated on orbital shaker

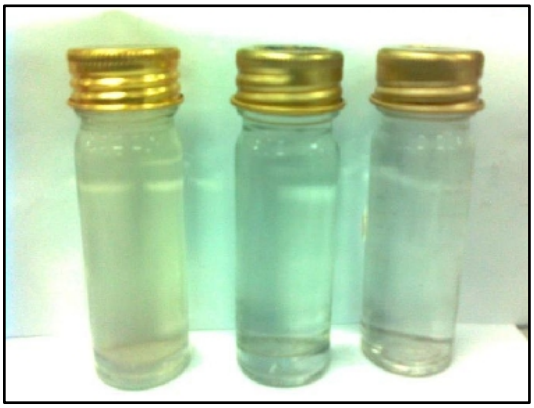

Appendix A5 Samples were ready for AAS analyze

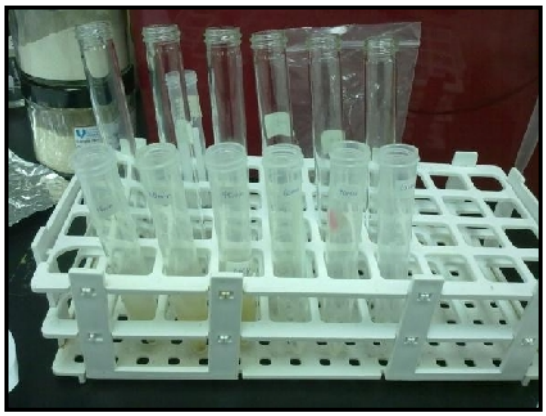

Appendix A3 Samples were ready for centrifuge

APPENDIX B Experimental Data

Appendix B1 Effect of initial concentration

Initial Concentration (kg/m^3)	Final Concentration (kg/m^3)	Percentage Removal (%)
0.01625	0.0004	97.54
0.03251	0.0080	75.39
0.04876	0.0118	75.80
0.06501	0.0196	69.85

Appendix B2 Effect of contact time at different initial concentration

(a) For 50mg/L

Time (min)	Initial Concentration (kg/m^3)	Final Concentration (kg/m^3)	Amount adsorbed, q(kg/kg)
0	0.01625	0.01625	0
1	0.01625	0.01274	0.00019
2	0.01625	0.09253	0.00057
3	0.01625	0.00763	0.00086
4	0.01625	0.00557	0.001068
5	0.01625	0.00548	0.001077
10	0.01625	0.00263	0.001362
15	0.01625	0.00234	0.001391
30	0.01625	0.00221	0.001404
45	0.01625	0.00199	0.001426
60	0.01625	0.00186	0.001439
90	0.01625	0.00181	0.001445
120	0.01625	0.00152	0.001473

(b) For 100mg/L

Time (min)	Initial Concentration (kg/m^3)	Final Concentration (kg/m^3)	Amount adsorbed, q(kg/kg)
0	0.03251	0.03251	0
1	0.03251	0.02318	0.000933
2	0.03251	0.01622	0.001629
3	0.03251	0.01585	0.001666
4	0.03251	0.01519	0.001732
5	0.03251	0.01471	0.001780
10	0.03251	0.01410	0.001841
15	0.03251	0.01346	0.001905
30	0.03251	0.01209	0.002042
45	0.03251	0.01126	0.002125
60	0.03251	0.00784	0.002467
90	0.03251	0.00737	0.002514
120	0.03251	0.00667	0.002584

(c) For 150mg/L

Time (min)	Initial Concentration (kg/m^3)	Final Concentration (kg/m^3)	Amount adsorbed, q(kg/kg)
0	0.04876	0.04876	0
1	0.04876	0.03667	0.001209
2	0.04876	0.03487	0.001390
3	0.04876	0.03195	0.001681
4	0.04876	0.02820	0.002056
5	0.04876	0.02436	0.002440
10	0.04876	0.02269	0.002607
15	0.04876	0.02138	0.002738
30	0.04876	0.01995	0.002881
45	0.04876	0.01899	0.002978
60	0.04876	0.01893	0.002983
90	0.04876	0.01762	0.003114
120	0.04876	0.01746	0.003130

(d) For 200mg/L

Time(min)	Initial Concentration (kg/m^3)	Final Concentration (kg/m^3)	Amount adsorbed, q(kg/kg)
0	0.06501	0.06501	0
1	0.06501	0.05219	0.001283
2	0.06501	0.04822	0.001680
3	0.06501	0.04430	0.002072
4	0.06501	0.03810	0.002691
5	0.06501	0.03528	0.002973
10	0.06501	0.03510	0.002991
15	0.06501	0.03492	0.003010
30	0.06501	0.03075	0.003426
45	0.06501	0.03032	0.003469
60	0.06501	0.02973	0.003528
90	0.06501	0.02955	0.003546
120	0.06501	0.02901	0.003601

Appendix B3 Effect of adsorbent dosage

Adsorbent dosage (g)	Initial concentration (kg/m^3)	Final concentration (kg/m^3)	Percentage Removal (%)
0.5	0.04876	0.03852	21.00
0.7	0.04876	0.02592	46.84
1	0.04876	0.01746	64.19

Appendix B4 Empirical relation for adsorbent dosage with % removal

Adsorbent dosage, m_a (g)	Percentage Removal, R (%)	$1/m_a$ (kg^{-1})	1/R (%)
0.5	21.00	2	0.048
0.7	46.84	1.428571	0.021
1.0	64.19	1	0.016

Appendix B5 Relative concentration of different manganese species at different pH at initial concentration 100 mg/L

pH	Mn^{2+}	$MnSO_4$	$MnHSO_4$	MnOH+	$Mn(OH)_2$
0	0.843434	0.079973	0.076593	5.28833E-11	5.32207E-16
1	0.843434	0.079973	0.076593	5.28833E-10	5.32207E-14
2	0.843434	0.079973	0.076593	5.28833E-09	5.32207E-12
3	0.843434	0.079973	0.076593	5.28833E-08	5.32207E-10
4	0.843434	0.079973	0.076593	5.28833E-07	5.32207E-08
5	0.843426	0.079972	0.076592	5.28828E-06	5.32202E-06
6	0.843007	0.079892	0.076516	5.28566E-05	0.000531938
7	0.80576	0.072988	0.069903	0.000505211	0.050843441
8	0.136124	0.002083	0.001995	0.000853499	0.858944062
9	0.001582	2.81E-07	2.7E-07	9.9199E-05	0.99831813
10	1.58E-05	2.82E-11	2.7E-11	9.93636E-06	0.999974601
11	1.59E-07	2.83E-15	2.71E-15	9.94955E-07	1.00130237
12	0	0	0	0	0
13	0	0	0	0	0
14	0	0	0	0	0

Appendix B6 Langmuir Isotherm parameters

Initial Concentration (mg/L)	Equilibrium Concentration (mg/L)	Amount adsorbed, q (kg/kg)	1/Ce (L/mg)	1/q (kg/kg)
0.0162535	0.0004	0.00158535	2500	630.77633
0.032507	0.008	0.0024507	125	408.04751
0.0487604	0.0118	0.00369604	84.74576271	270.55962
0.0650139	0.0196	0.00454139	51.02040816	220.1969

Appendix B7 Pseudo first order and second order kinetic

Time (min)	Initial concentration (mg/L)	Final Concentration (mg/L)	Qt	qe-qt	Log (qe-qt)	t/qt
0	0.0650	0.0650	0	0.0298	-1.5257	0
1	0.0650	0.0522	0.00128	0.0285	-1.5448	779.55
2	0.0650	0.0482	0.00167	0.0281	-1.5509	1190.65
3	0.0650	0.0443	0.00207	0.0277	-1.5570	1448.16
4	0.0650	0.0381	0.00269	0.0271	-1.5668	1486.38
5	0.0650	0.0353	0.00297	0.0268	-1.5714	1681.64
10	0.0650	0.03519	0.00299	0.0268	-1.5717	3342.91
15	0.0650	0.0349	0.00300	0.0267	-1.5720	4984.17
30	0.0650	0.0308	0.00342	0.0263	-1.5788	8756.07
45	0.0650	0.0303	0.00346	0.0263	-1.5795	12971.21
60	0.0650	0.0297	0.00352	0.0262	-1.5805	17006.335
90	0.0650	0.0296	0.00354	0.0262	-1.5808	25379.18
120	0.0650	0.0290	0.00360	0.0261	-1.5817	33328.13

Appendix B8 The experimental and theoretical Value for Langmuir model at initial concentration of 50 mg/L

Time(min)	q(experimental), kg/kg	q (theoretical), kg/kg
0	0	0.001497
1	0.000186	0.007529
2	0.000568	0.007528
3	0.000862	0.007527
4	0.001068	0.007527
5	0.001077	0.007527
10	0.001362	0.007526
15	0.001391	0.007526
30	0.001404	0.007526
45	0.001426	0.007526
60	0.001439	0.007526
90	0.001444	0.007526
120	0.001473	0.007526

Appendix B9 Modified Langmuir Isotherm Curve

Initial concentration (mg/L)	Equilibrium concentration, Ce (mg/L)	Amount adsorbed, q (kg/kg)	$\sqrt{\frac{q}{C_e}}$
0.01625	0.0004	0.00158535	1.990821439
0.03251	0.008	0.0024507	0.553477077
0.04876	0.0118	0.00369604	0.55966417
0.06501	0.0196	0.00454139	0.481355972

Appendix B10 Plot for determination of k_1 of the system

Initial (mg/L)	Initial concentration (mg/L)	dq/dt
50	0.01625	0.0004
100	0.03251	0.0011
150	0.04876	0.0017
200	0.06501	0.0015

Appendix B11 Comparison between the experimental and theoretical value

(a)50mg/L

Time (min)	dq/dt (experimental)	dq/dt (Dual site)	dq/dt (Langmuir)
0	0.00036	0.00076	0.12265608
1	0.00028	0.00067	0.10480628
2	0.00017	0.00049	0.07041762
3	0.00013	0.00036	0.0460666
4	0.00011	0.00026	0.03016158
5	0.00014	0.00026	0.02952134
10	0.00005	0.00012	0.00904418
15	0.00002	0.00011	0.00710104
30	0.00002	0.00010	0.00619272
45	0.00001	0.00009	0.00472504
60	0.00001	0.00009	0.00382699
90	0.00001	0.00008	0.00349122
120	0.00000	0.00007	0.00159894

(b) 100mg/L

Time(min)	dq/dt (experimental)	dq/dt (Dual site)	dq/dt (Langmuir)
0	0.00053	0.00152	0.133850026
1	0.00041	0.00108	0.080002028
2	0.00028	0.00075	0.046582893
3	0.00022	0.00074	0.044976902
4	0.00018	0.00071	0.042125991
5	0.00009	0.00068	0.040100853
10	0.00006	0.00065	0.037561468
15	0.00003	0.00062	0.034939259
30	0.00002	0.00056	0.029475146
45	0.00002	0.00052	0.026292249
60	0.00001	0.00036	0.013974589
90	0.00001	0.00034	0.012399242
120	0.00000	0.00031	0.010084998

(c) 150mg/L

Time (min)	dq/dt (experimental)	dq/dt (Dual site)	dq/dt (Langmuir)
0	0.00086	0.00227	0.146178586
1	0.00035	0.00170	0.088335025
2	0.00028	0.00162	0.080778786
3	0.00026	0.00148	0.069185328
4	0.00024	0.00131	0.055323499
5	0.00013	0.00113	0.042408048
10	0.00009	0.00105	0.037188338
15	0.00005	0.00099	0.03327763
30	0.00003	0.00092	0.029163529
45	0.00002	0.00088	0.026490668
60	0.00002	0.00088	0.026320982
90	0.00001	0.00082	0.022834748
120	0.00000	0.00081	0.022418243

(d) 200mg/L

Time(min)	dq/dt (Experimental)	dq/dt (Dual Site)	dq/dt (Langmuir)
0	0.00074	0.00303	0.151081606
1	0.00042	0.00243	0.096832543
2	0.00035	0.00224	0.082280176
3	0.00034	0.00206	0.068951523
4	0.00030	0.00177	0.049978653
5	0.00015	0.00163	0.042189224
10	0.00010	0.00163	0.0417074
15	0.00006	0.00162	0.041227777
30	0.00004	0.00142	0.03080365
45	0.00003	0.00140	0.029793541
60	0.00002	0.00138	0.028431398
90	0.00002	0.00137	0.028016953
120	0.00000	0.00134	0.026786817